Journal of Hydrology 640 (2024) 131661

Contents lists available at ScienceDirect

Journal of Hydrology

journal homepage: www.elsevier.com/locate/jhydrol

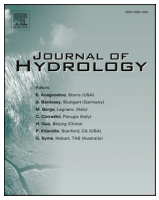

Research papers

Trends of meteorological and hydrological droughts and associated parameters using innovative approaches

Ahmad Abu Arra [a,b,*], Sadık Alashan [c,**], Eyüp Şişman [a,d,***]

[a] Department of Civil Engineering, Yildiz Technical University, Istanbul, Türkiye
[b] Department of Civil and Architectural Engineering, An-Najah National University, Nablus, Palestine
[c] Department of Civil Engineering, Bingöl University, Bingöl, Türkiye
[d] Department of Civil Engineering, School of Engineering and Natural Sciences, Istanbul Medipol University, Istanbul, Türkiye

ARTICLE INFO

This manuscript was handled by Corrado Corradini, Editor-in-Chief

Keywords:
Time series
Trend analysis
Drought indices
Standardized Precipitation Index (SPI)
Standardized Precipitation Evapotranspiration Index (SPEI)
Streamflow Drought Index (SDI)
Innovative Polygon Trend Analysis (IPTA)
Climate change

ABSTRACT

Climate change and drought have profound effects on hydro-meteorological series. In addition to spatial, these effects could be on annual, seasonal, monthly, or daily temporal scales. In the literature, seasonal Mann-Kendall and Kendall Tau, Standardized Precipitation Index (SPI), Standardized Precipitation Evapotranspiration Index (SPEI), and Standardized Runoff Index are mostly used to detect seasonal effects (autumn, winter, spring, and summer), despite some restrictive assumption. Innovative Polygon Trend Analysis (IPTA) method developed from Innovative Trend Analysis (ITA) analyzes monthly effects on hydro-meteorological variables without restrictive assumptions. In this study, the IPTA method is revised and developed as Periodic Innovative Polygon Trend analysis (P-IPTA) to analyze hydro-meteorological series in periods of 1, 3, 6, 9, and 12 months instead of one-month duration. The method turns to the IPTA for one-month evaluations. Also, ITA method is improved by adding the frequencies for each drought classification (F-ITA). For the precipitation and water availability (Istanbul, Türkiye) and stream flow (Danube River, Romania) series, the P-IPTA method has been used in addition to the SPI, SPEI, and SDI methods to detect the trends in meteorological and hydrological droughts, and their associated parameters. There are generally decreasing trends, increasing drought frequencies, and decreasing wet event frequencies in the study areas. As the period lengths of the hydro-meteorological series increase, drought becomes more evident. Unlike these methods, the method results are consistent with the F-ITA SPI, SPEI, and SDI graphs and can give drought and wet periods. Similarly, the new P-IPTA method will enable researchers to investigate seasonal effects not only on hydro-meteorological series but also on any variable.

1. Introduction

Presently, scientists are increasingly focusing on the effects of climate change due to the rise in the intensity and occurrence of extreme events like droughts, heatwaves, sandstorms, wildfires, and floods (Alashan 2020a; Benzater et al. 2019; Abu Arra and Şişman 2024). Among these, drought stands out due to its prolonged onset, long duration, and wide-ranging consequences, which are generated primarily by natural climate pattern drivers (Danandeh Mehr and Vaheddoost 2020; Mishra and Singh 2010). This cyclical phenomenon ranks among the most complex natural disasters globally due to its slow development, lasting effects, and frequent occurrence (Lai et al. 2019; Salim et al. 2023). Droughts impact both water supply and demand due to reduced precipitation, influencing various sectors, including the economy, industry, and agriculture (Abu Arra and Şişman 2023; Du et al. 2021). As per data from the International Disaster Database (EM-DAT), worldwide financial losses due to drought amounted to approximately 221 billion dollars between 1960 and 2016 (Tong et al. 2018). According to Wu et al. (2021), it has been shown that the annual economic losses due to drought disasters on a global scale have reached an estimated 6–8 billion dollars.

Drought monitoring typically encompasses four distinct categories:

* Corresponding author at: Department of Civil Engineering, Yildiz Technical University, Istanbul, Türkiye.
** Corresponding author.
*** Corresponding author.
E-mail addresses: ahmad.arra@std.yildiz.edu.tr, s11419527@stu.najah.edu (A. Abu Arra), sadikalashan@bingol.edu.tr (S. Alashan), esisman@yildiz.edu.tr, esisman@medipol.edu.tr (E. Şişman).

https://doi.org/10.1016/j.jhydrol.2024.131661
Received 1 May 2024; Received in revised form 15 June 2024; Accepted 28 June 2024
Available online 17 July 2024

meteorological, agricultural, hydrological, and socioeconomic droughts (Wilhite 2000). Each category has specific associated parameters and indices. Various drought indices, as a first step, have been developed to facilitate drought calculations, including Standardized Precipitation Index (SPI) (McKee et al. 1993), Reconnaissance Drought Index (RDI) (Tsakiris et al. 2007), Streamflow Drought Index (SDI) (Nalbantis and Tsakiris 2009), and Standardized Precipitation Evapotranspiration Index (SPEI) (Vicente-Serrano et al. 2010). Understanding the mechanism and parameters of each drought index is crucial in drought and climate change studies (Wu et al. 2024; Birpınar et al. 2023). Different drought indices rely on specific inputs to assess drought conditions accurately. For instance, the SPI utilizes precipitation records as its primary driving factor. On the other hand, SPEI incorporates the difference between precipitation and evapotranspiration to evaluate the drought index. SDI also relies on runoff records as its key parameter. Recognizing these distinctions enables researchers to effectively interpret and compare drought assessments across various regions and time periods, contributing to a more comprehensive understanding of drought dynamics and their implications for climate change adaptation and mitigation efforts.

Climate change significantly influences water resources, with climatic factors like precipitation and temperature playing a pivotal role in the global hydrological cycle (Tsakiris and Loucks 2023). Changes in these elements can lead to shifts in water resources on both a global and regional scale (Katipoğlu 2022; Şan et al. 2024). Precipitation plays a vital role in replenishing surface water and is a key element of the hydrological cycle. Altered precipitation patterns, attributed to climate change, can exacerbate severe drought events (Şişman and Kizilöz 2021; Güçlü et al. 2020). In addition to identifying and analyzing various drought types, assessing the drought trend is crucial for managing and determining the timing and extent of necessary precautions.

Various trend analysis methods are available, encompassing both traditional and innovative approaches. Among the traditional methods are the Mann-Kendall (MK) method (Mann, 1945; Kendall, 1975) and Sen's slope method (Sen, 1968). However, these conventional trend analysis methods have some limitations. These methods require a minimum duration of data, typically in terms of time, and assume independence without considering any serial correlation, which limits the ability to make sequential comparisons among different segments within the same dataset (Güçlü 2018; Koycegiz 2024). Conversely, innovative trend analysis methods offer the advantage of capturing periodic changes, including variations at monthly and daily intervals (Alashan 2020b; Şen et al. 2019). Şen et al. (2019) introduced an enhanced approach termed Innovative Polygon Trend Analysis (IPTA), designed to refine the Innovative Trend Analysis (ITA) method. IPTA not only identifies trends within a given dataset but also constructs a trend polygon, facilitating improved linguistic and numerical interpretation and assisting in identifying seasonal trend shifts, seasonal transition slope, and seasonal transition lengths across successive segments extracted from the original hydro-meteorological time series (Kesgin et al. 2024). Various studies investigating drought trend analysis have been conducted, including research by Gumus et al. (2021), Nouri and Homaee (2020), Elouissi et al. (2021), Yeşilköy and Şaylan (2022), Berhail and Katipoğlu (2023), Kartal and Emiroglu (2024), and Simsek et al. (2024).

In drought studies, most research has predominantly focused on the temporal and spatial evaluation of drought conditions. Recently, trend analysis investigations have been extensively employed to examine various hydro-meteorological variables, including precipitation and temperature, and evaluate drought utilizing both classical and innovative trend methods. However, a noticeable gap exists in the literature, where comprehensive research covering drought indices, drought frequencies, and their associated parameters in trend analysis remains scarce. In order to address this gap and provide a comprehensive view of drought and associated parameters, new concept and framework with innovative approaches are being suggested. These include investigating the relationship between drought and its associated parameters, aiming to offer a more holistic understanding of drought dynamics. The objectives of this research are: 1) introducing the the proposed novel Periodic Innovative Polygon Trend Analysis method (P-IPTA) to evaluate temporal trends in hydro-meteorological parameters across a range of timescales; 2) identifying trends in different meteorological and hydrological drought indices (SPI, SPEI, SDI) across different time scales using the newly improved Frequency Innovative Trend Analysis (F-ITA), incorporating drought classification frequencies to better understand the drought trends; and finally 3) exploring the relationships between trends in meteorological and hydrological drought indices and their associated parameters. These innovative trend methods and new concept will provide a holistic understanding of droughts and associated parameters' trends at varying time scales. This work not only addresses a critical gap in current drought and trend research methodologies but also sets the stage for enhanced strategies in managing droughts under changing climate conditions.

2. Methodology

The methodology section includes data collection of hydrometeorological variables such as precipitation, temperature, and streamflow for various applications. Meteorological and hydrological drought indices, including the SPI, SPEI, and SDI, are then calculated at different timescales. The trends of these drought indices are analyzed using the improved F-ITA method, which incorporates the frequencies of each drought classification. Simultaneously, periodic and seasonal trends of the parameters associated with these drought indices are calculated using the proposed P-IPTA method. Employing both F-ITA and P-IPTA methods enables a comprehensive comparison and investigation of the relationships between the trends of drought indices and their associated parameters. Finally, this research utilizes the innovative monthly trend chart to determine trends within all months in a single graph, clearly visualizing temporal and spatial changes.

2.1. Standardized precipitation index (SPI)

SPI, developed by McKee et al. (1993), assesses meteorological drought across various timescales, like 3-month, 6-month, 12-month, and 24-month durations, solely relying on precipitation data. Initially, the original monthly precipitation data undergoes fitting to an appropriate probability density function (PDF). The selection of the PDF involves scrutinizing the goodness-of-fit tests, such as Chi-Square and Kolmogorov-Smirnov tests, applied to the original precipitation records for any timescale. Subsequently, probabilities are computed from the monthly precipitation data and probabilistically standardized to a standard normal PDF with a mean of zero and a standard deviation of one. In this research, the Kolmogorov-Smirnov test is used for all datasets and time scales.

2.2. Standardized precipitation evapotranspiration index (SPEI)

Vicente-Serrano et al. (2010) introduced the SPEI, which is similar to the SPI method but incorporates potential evapotranspiration (PET) data. PET estimation can employ various methods like the Thornthwaite method (Thornthwaite, 1948). In this research, the PET estimation employs the Thornthwaite method. The Thornthwaite method derives PET from average monthly temperature records. SPEI primarily depends on the difference between precipitation and PET data (Water Availability (Water Balance) – WA), which are fitted to the appropriate probability density function (PDF). Following assessment with Chi-Square and Kolmogorov-Smirnov tests, probabilities from the chosen PDF are computed for water availability records for any time scale. These probabilities are then probabilistically standardized into a

standard normal PDF. Additional insights into the SPEI method can be found in the original study by Vicente-Serrano et al. (2010).

2.3. Streamflow drought index (SDI)

This drought index proposed by Nalbantis and Tsakiris (2009) shares similarities with the SPI and SPEI indices, with a key distinction being the inclusion of monthly streamflow data in its computation instead of precipitation and water availability to determine drought index. The SDI is utilized to monitor and identify drought events at a specific gauge. It is widely accessible and user-friendly. Additionally, the accuracy of the results improves with longer streamflow records. Similar to the SPI, it allows for examination across various timescales.

2.4. Drought Classification

McKee et al. (1993) introduced the classification outlined in Table 1 to categorize drought conditions based on index values. This classification scheme assigns specific labels to different ranges of index values, such as "moderate drought," "severe drought," and "extreme drought," each reflecting varying degrees of water deficit and its impact on the environment. The simplicity and practicality of this classification have led to its widespread adoption in the literature, making it one of the most frequently utilized classifications for assessing and monitoring drought. Adopting a universally accepted drought classification facilitates the comparison processes, effective water resources management, and climate change mitigation and adaptation strategies. Furthermore, employing standardized metrics allows for a symmetric approach, enabling assessment and monitoring of both wet and dry climates using consistent drought indices.

2.5. Frequency – innovative trend analysis (F – ITA)

The ITA methodology, which has been generally used to determine holistic and partial trends in hydro-meteorological data in the last decade and has been frequently used to define trends in drought indices time series in recent years, was proposed by Şen (2012). Compared to classical trend methods, the most important advantages of the ITA method are its simplification and its ability to be directly used as it does not rely on assumptions of serial independence, normality, or large sample sizes. It utilizes a comparison of scatter points on a Cartesian coordinate system based on the 1:1 (45°) line, which allows for a more flexible and robust analysis of trends in hydro-meteorological time series. The ITA method has been enhanced by incorporating the frequency of drought classification for each half, providing a simplified and comprehensive overview of changing drought frequencies. For example, it reveals that extreme drought events may rise from 5 % in the first half to 10 % in the second half, indicating a twofold increase in extreme drought events. The geometric definitions of trends can be made and visually interpreted easily with the help of graphs. Monotonic increasing and decreasing trends and non-monotonic increasing and decreasing trends with the frequency of each drought classification can be defined based on F-ITA graphs, and non-monotonic and partial trends can not be entirely used in classical methods.

Table 1
Drought classification according to McKee et al. (1993).

(Drought Index value_DI)	Drought classification	Probability (%)
$2.00 \leq DI$	Extreme wet (EW)	2.3 %
$1.50 \leq DI < 2.00$	Severe wet (SW)	4.4 %
$1.00 \leq DI < 1.50$	Moderate wet (MW)	9.2 %
$-1.00 < DI < 1.00$	Normal (N)	68.2 %
$-1.50 \leq DI \leq -1.00$	Moderate drought (MD)	9.2 %
$-2.00 < DI \leq -1.50$	Severe drought (SD)	4.4 %
$-2.00 \geq DI$	Extreme drought (ED)	2.3 %

2.6. Periodic – innovative polygon trend analysis (P – IPTA)

Climate change has periodic or seasonal effects on hydro-meteorological events, including precipitation, temperature, evaporation, evapotranspiration, groundwater flow, and runflow. Mann-Kendall (MK) method is frequently used in the literature to detect holistic monotonic trends in non-periodic monthly and annual time series (Mann (1945) and Kendall (1948)). Helsel and Frans (2006) modified the MK method and named the Seasonal Kendall Test (SKT) to detect monotonic trends in seasonal time series. Although researchers very intensely use these methods, they have notable restrictions on the requirement for serial independence and long data length (Von Storch 1995; Yue et al. 2002). Şen (2012) proposed a new trend detection method called Innovative Trend Analyses (Şen_ITA), which does not rely on any restrictive assumption. The method is applied to monthly and annual time series to detect both monotonic and non-monotonic holistic and partial trends visually and statistically (Şen 2014; Alashan 2020b; Serinaldi et al. 2020). The same author, along with colleagues, have revised Şen_ITA method with the aim of calculating seasonal transition slopes and lengths and obtaining a polygon that illustrates transitions among months (Şen et al. 2019). As a result of the introduction of this polygon, the method is named Innovative Polygon Trend Analysis (IPTA), and there has been extensive research related to the method (Şan et al. 2021; Yenice and Yaqub 2022; Gupta and Chavan 2023; Eren and Yaqub 2024). The IPTA method generally uses a 1-month timescale to calculate transition slopes and lengths and detect trends among months (Fig. 1). In this figure, the 1:1 line represents a trendless line, scatter points represent average monthly precipitation values, and the green lines depict 5 % trend lines. If scatter points lie above (below) the 1:1 trendless line, it indicates an increasing (decreasing) tendency. For brevity, in this study, months with scatter points lying within the 5 % trendlines are considered as trendless.

In this study, the IPTA method is enhanced to analyze seasonal time series with different cumulative or average timescales such as 1-month, 3-months, 6-months, 9-months, 12-months, 24-months, etc. The new improved method is named periodic innovative polygon trend analysis (P-IPTA). Cumulative series are typically more compatible with precipitation, evaporation, and evapotranspiration data, whereas average series are often preferred for streamflow, flow, and temperature data in hydro-meteorology. Average seasonal series are calculated using Equation1, where *ts* represents the timescale (e.g., 1, 3, 6, 9, 12, etc.), $Z_{\left(\left\lfloor 1+\frac{j+ts-2}{12}\right\rfloor, j\right)}$ denotes the monthly time series according to the speci-

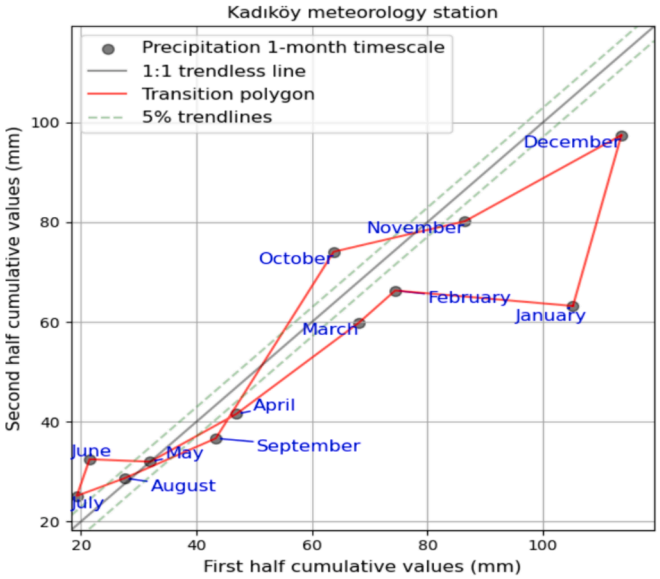

Fig. 1. The application of the IPTA method for Kadıköy precipitation series.

fied timescale, *ts*, and data length, n. The parameter j varies from 1 to 12, when $ts = 1$ and $j = 12$.

$$\begin{bmatrix} \frac{1}{ts}\sum_{j=1}^{mod(j+ts-1,12)} Z_{\left(\left\lfloor 1+\frac{j+ts-2}{12}\right\rfloor, j\right)} & \frac{1}{ts}\sum_{j=2}^{mod(j+ts-1,12)} Z_{\left(\left\lfloor 1+\frac{j+ts-2}{12}\right\rfloor, j\right)} & \cdots & \frac{1}{ts}\sum_{j=12}^{mod(j+ts-1,12)} Z_{\left(\left\lfloor 1+\frac{j+ts-2}{12}\right\rfloor, j\right)} \\ \frac{1}{ts}\sum_{j=1}^{mod(j+ts-1,12)} Z_{\left(\left\lfloor 2+\frac{j+ts-2}{12}\right\rfloor, j\right)} & \frac{1}{ts}\sum_{j=2}^{mod(j+ts-1,12)} Z_{\left(\left\lfloor 2+\frac{j+ts-2}{12}\right\rfloor, j\right)} & \cdots & \frac{1}{ts}\sum_{j=12}^{mod(j+ts-1,12)} Z_{\left(\left\lfloor 2+\frac{j+ts-2}{12}\right\rfloor, j\right)} \\ \vdots & \vdots & & \vdots \\ \vdots & \vdots & & \vdots \\ \frac{1}{ts}\sum_{j=1}^{mod(j+ts-1,12)} Z_{\left(\left\lfloor i+\frac{j+ts-2}{12}\right\rfloor, j\right)} & \frac{1}{ts}\sum_{j=2}^{mod(j+ts-1,12)} Z_{\left(\left\lfloor i+\frac{j+ts-2}{12}\right\rfloor, j\right)} & \cdots & \frac{1}{ts}\sum_{j=12}^{mod(j+ts-1,12)} Z_{\left(\left\lfloor i+\frac{j+ts-2}{12}\right\rfloor, j\right)} \\ \vdots & \vdots & & \vdots \\ \vdots & \vdots & & \vdots \\ \frac{1}{ts}\sum_{j=1}^{mod(j+ts-1,12)} Z_{\left(\left\lfloor n+\frac{j+ts-2}{12}\right\rfloor, j\right)} & \frac{1}{ts}\sum_{j=2}^{mod(j+ts-1,12)} Z_{\left(\left\lfloor n+\frac{j+ts-2}{12}\right\rfloor, j\right)} & \cdots & \frac{1}{ts}\sum_{j=12}^{mod(j+ts-1,12)} Z_{\left(\left\lfloor n+\frac{j+ts-2}{12}\right\rfloor, j\right)} \end{bmatrix} \quad (1)$$

representing the total number of months in a year, while 'i' ranges from 1 to 'n'; representing the length of the data. The floor function ($\left\lfloor 1+\frac{j+ts-2}{12}\right\rfloor$) rounds a given real number down to the nearest integer that is less than or equal to itself. For example, $Z_{\left(\left\lfloor 1+\frac{j+ts-2}{12}\right\rfloor, 12\right)} = Z_{(1,12)}$ corresponds to a series value belonging to the first year and twelfth month

Using the similar process to obtain cumulative seasonal series, Equation (2) is applied, resulting the total seasonal time series for certain timescales. Equations (1) and (2) are presented in matrix form to help readers understand the mathematical process better.

$$\begin{bmatrix} \sum_{j=1}^{mod(j+ts-1,12)} Z_{\left(\left\lfloor 1+\frac{j+ts-2}{12}\right\rfloor, j\right)} & \sum_{j=2}^{mod(j+ts-1,12)} Z_{\left(\left\lfloor 1+\frac{j+ts-2}{12}\right\rfloor, j\right)} & \cdots & \sum_{j=12}^{mod(j+ts-1,12)} Z_{\left(\left\lfloor 1+\frac{j+ts-2}{12}\right\rfloor, j\right)} \\ \sum_{j=1}^{mod(j+ts-1,12)} Z_{\left(\left\lfloor 2+\frac{j+ts-2}{12}\right\rfloor, j\right)} & \sum_{j=2}^{mod(j+ts-1,12)} Z_{\left(\left\lfloor 2+\frac{j+ts-2}{12}\right\rfloor, j\right)} & \cdots & \sum_{j=12}^{mod(j+ts-1,12)} Z_{\left(\left\lfloor 2+\frac{j+ts-2}{12}\right\rfloor, j\right)} \\ \vdots & \vdots & & \vdots \\ \vdots & \vdots & & \vdots \\ \sum_{j=1}^{mod(j+ts-1,12)} Z_{\left(\left\lfloor i+\frac{j+ts-2}{12}\right\rfloor, j\right)} & \sum_{j=2}^{mod(j+ts-1,12)} Z_{\left(\left\lfloor i+\frac{j+ts-2}{12}\right\rfloor, j\right)} & \cdots & \sum_{j=12}^{mod(j+ts-1,12)} Z_{\left(\left\lfloor i+\frac{j+ts-2}{12}\right\rfloor, j\right)} \\ \vdots & \vdots & & \vdots \\ \vdots & \vdots & & \vdots \\ \sum_{j=1}^{mod(j+ts-1,12)} Z_{\left(\left\lfloor n+\frac{j+ts-2}{12}\right\rfloor, j\right)} & \sum_{j=2}^{mod(j+ts-1,12)} Z_{\left(\left\lfloor n+\frac{j+ts-2}{12}\right\rfloor, j\right)} & \cdots & \sum_{j=12}^{mod(j+ts-1,12)} Z_{\left(\left\lfloor n+\frac{j+ts-2}{12}\right\rfloor, j\right)} \end{bmatrix} \quad (2)$$

To enhance understanding of the new method, the application steps are outlined as follows, with detailed explanations provided for each step.

Step-1: Select the timescale.

- The IPTA method utilizes 1-month timescale.
- Seasons corresponding to 1-month timescales are defined as Jan, Feb, Mar, ……, Dec.
- Other available timescales include 1-month, 3-months, 6-months, 9-months, 12-months, 24-months, etc.

Step-2: Determine seasons according to selected timescales.

- Based on the chosen timescale, determine the seasons accordingly.
- For a 3-months timescale, seasons result in periods such as Jan-Mar (from January to March), Feb-Apr, Mar-May, …, Dec-Feb;
- For a 6-months timescale, seasons correspond to periods like Jan-Jun, Feb-Jul, Mar-Aug, …, Dec-May, and so on.

Step-3: Calculate the cumulative or average of seasonal series.

- For the cumulative series, sum the values for each season.
- For the average series, calculate the mean of each season.

Step-4: Apply the innovative trend analysis techniques to seasonal cumulative and average series.

- The resulting seasonal cumulative or average series is divided into equal half series.
- The averages of these two halves series are calculated.
- The average of the first half (second half) for the seasonal series is drawn on the horizontal(vertical) axis.
- A 1:1 trendless line is plotted on the same graph.

Step-5: Draw the periodic innovative trend polygon.

- The resulting scatter points are connected by lines, forming a polygon referred to as the periodic innovative trend polygon (P-IPTA).
- A polygon with a single loop is classified as a regular polygon, whereas a polygon with multiple loops is classified as an irregular polygon.

Step-6: Calculate seasonal transition trend lengths and slopes based on successive scatter points.

- The lengths of the line connecting successive scatter points yield seasonal transitional lengths (Equation (3), while the slopes of the line represent seasonal transitional slopes (Equation (4).

$$Seasonaltransitionlength = \sqrt{(y_{j+1} - y_j)^2 + (x_{j+1} - x_j)^2} \tag{3}$$

$$Seasonaltransitionslope = \frac{(y_{j+1} - y_j)}{(x_{j+1} - x_j)} 1 \le j \le 12 \tag{4}$$

2.7. Mann-Kendall test and Sen's slope estimator

The Mann-Kendall test is a non-parametric statistical method proposed to identify trends in time series data. It is particularly effective for detecting monotonic trends, whether they are increasing or decreasing. Initially introduced by Mann in 1945 (Mann 1945) and subsequently refined by Kendall in 1975 (Kendall 1975). The Mann-Kendall test statistic S is determined based on based on the ranks of the data points. A high positive value of S indicates an increasing trend, whereas a high negative value suggests a decreasing trend. It is calculated as:

$$S = \sum_{k=1}^{n-1} \sum_{j=k+1}^{n} sgn(x_j - x_k) \tag{5}$$

where:

x_i and x_j are data values (j > i). The sgn gives a value of + 1 when (x_j − x_i) > 0, 0 when (x_j − x_i) = 0, and −1 when (x_j − x_i) < 0.

S is obtained by multiplying the sgn results for all (x_i, x_j) data.

The variance of S is calculated to evaluate the statistical significance as:

$$Var(S) = \frac{n(n-1)(2n+5) - \sum_{i=1}^{m} t_i(t_i-1)(2t_i+5)}{18} \tag{6}$$

where n is the data numbers, m is the data numbers with the same value (tied groups), and t_i is the number of groups of the size t_i.

The Mann-Kendall Z statistic evaluates the statistical significance of a trend observed in a time series dataset. This statistic is computed as follows:

$$Z = \begin{cases} \frac{S-1}{\sqrt{Var(S)}}; S > 0 \\ 0; S = 0 \\ \frac{S+1}{\sqrt{Var(S)}}; S < 0 \end{cases} \tag{7}$$

On the other hand, Sen's slope is a non-parametric method for estimating slopes of a linear trend. was introduced independently by Theil (1950) and Sen (1968) (Theil 1950; Sen 1968). For a sample of n pairs, the slope is calculated as:

$$SS_i = \frac{x_j - x_k}{j - k} \tag{8}$$

where x_j and x_k are the data values, the slope is calculated for each data pair (i = 1,2,…,n) when j > i.

The SS_i values are sorted from small to large values, and the median of the values is accepted as the Sen's Slope. The median is calculated as:

$$SS_{med} = \begin{cases} SS_{[(n+1)/2],} \\ (SS_{[n/2]} + SS_{[(n+2)/2]})/2 \end{cases} \tag{9}$$

If n is odd, the first part of the equation is used. If there is an even number of n pairs, the mean of the two midmost slopes is calculated as described in the second equation.

2.8. Innovative monthly trend Chart

One of the most significant strengths of both IPTA and the proposed P-IPTA method lies in their ability to accurately identify trends, transitional trend slopes, and transitional trend lengths at various single and cumulative timescales. IPTA focuses on analyzing trends at a 1-month timescale, enabling the detection of trends among months based on a monthly scale. This approach allows for determining whether a trend exists, its transitional trend slope, and its length for each month. Similarly, P-IPTA extends this capability to any period or cumulative timescale, providing a more comprehensive analysis of trend patterns over longer durations. Furthermore, this study introduces the innovative monthly trend chart to enhance the presentation of these innovative polygon trend analyses. This chart clearly shows trend changes across all months or cumulative periods and for all stations within the study area or region, indicating whether there is a decreasing trend, increasing trend, or no trend for each month or cumulative timescale. Its simplicity not only improves the clarity of the presentation but also facilitates the mapping of innovative polygon trend analysis methods, enhancing their utility for spatial analysis and interpretation. Each number in the chart is the month, and the red color indicates an increasing trend, the green color indicates a decreasing trend, and black indicates no trend. Fig. 2 below shows the Innovative Monthly Trend Chart. Fig. 3 summarizes the main procedure used in this research.

3. Study area and application

To address the primary objectives of this study, the P-IPTA with F-

Fig. 2. Innovative Monthly Trend Chart (red color indicates an increasing trend, green color indicates a decreasing trend, and black indicates no trend). (For interpretation of the references to color in this figure legend, the reader is referred to the web version of this article.)

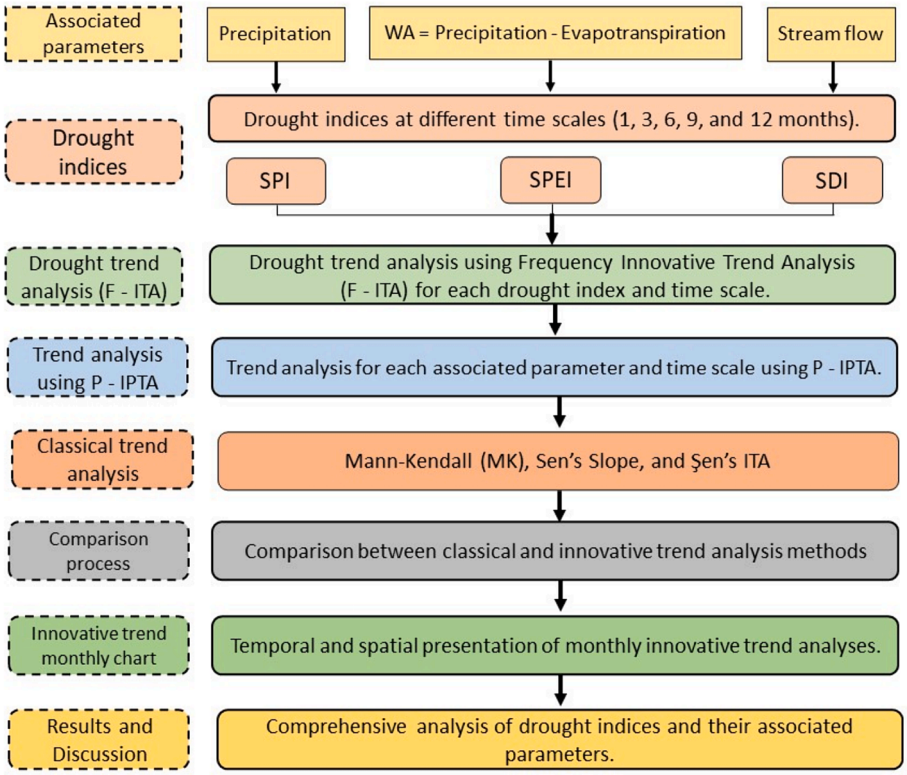

Fig. 3. Methodological approach.

ITA method was employed to analyze trends in meteorological and hydrological drought indices at five different timescales (1–3-6–9- and 12 months) and their associated parameters, including precipitation (P), water availability (WA), and streamflow data. Two distinct meteorological stations were selected as an application. The first station, Kadıköy Meteorological Station in Istanbul, Türkiye, was chosen for its availability of precipitation and temperature data, which were collected from the Turkish State Meteorological Service (MGM). Istanbul has a Mediterranean climate characterized by hot, dry summers and mild, wet winters. This station is applied for SPI and SPEI for the period between

Table 2
Statistical information about the temperature and cumulative precipitation series of the Kadıköy station and cumulative streamflow data for Nagymaros station at the Danube River.

Timescales	Cumulative Precipitation (mm)			Average Temperature (°C)			Cumulative Streamflow (m^3/s)		
	Mean	Std Dev	Skewness	Mean	Std Dev	Skewness	Mean	Std Dev	Skewness
1-months	55.74	27.43	0.369	14.64	6.67	0.074	2326.68	865.94	0.91
3-months	167.24	74.01	0.208	14.63	6.16	0.098	6980.74	2140.35	0.62
6-months	334.90	104.23	0.007	14.63	4.36	0.002	13960.50	3347.64	0.48
9-months	502.74	74.92	−0.208	14.62	2.06	−0.096	20942.52	3923.18	0.48
12-months	670.72	1.30	−1.39	14.62	0.01	1.172	27929.86	4470.15	0.44

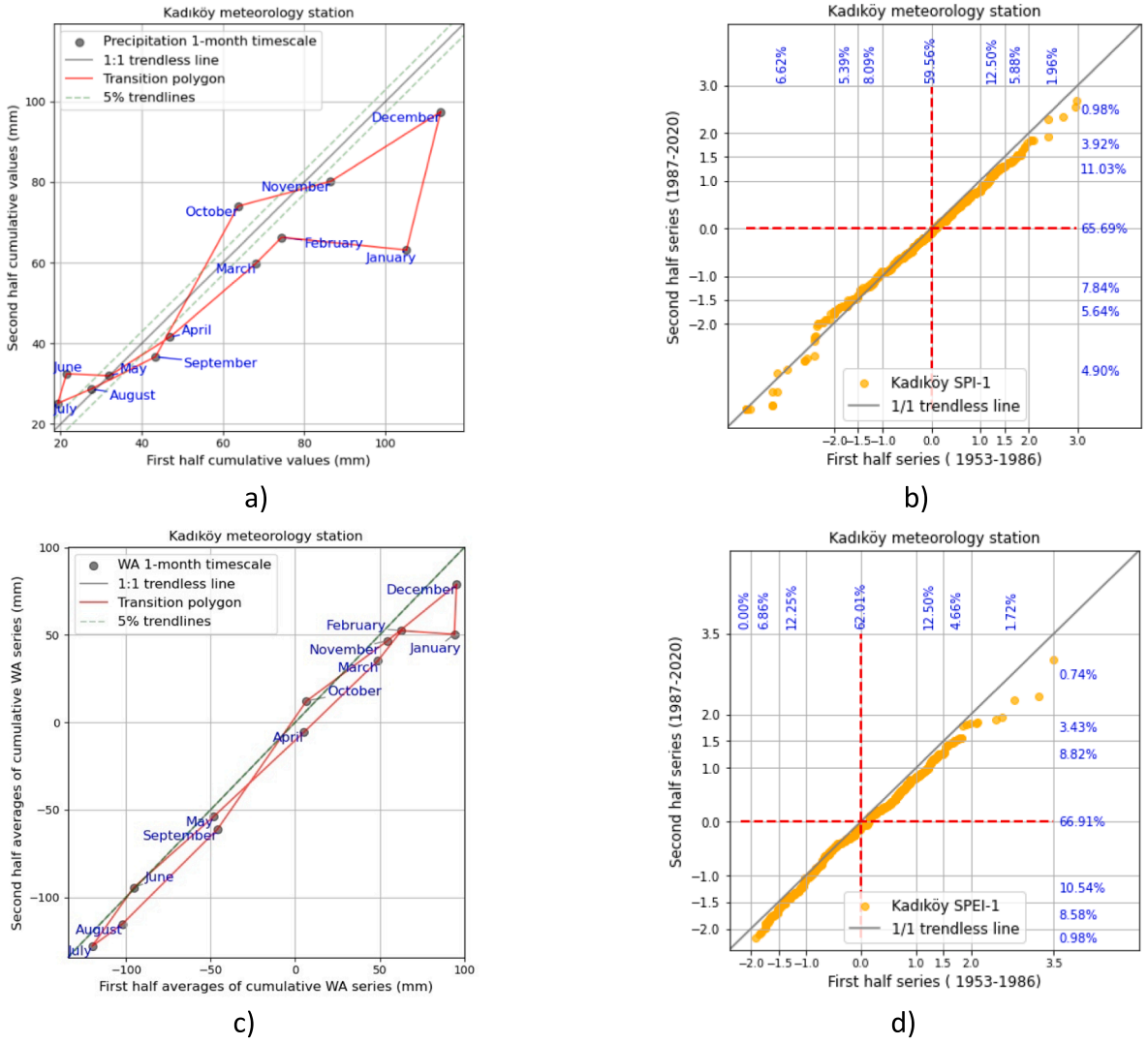

Fig. 4. IPTA and F-ITA graphs for Kadıköy station at a 1-month timescale. a) IPTA for precipitation, b) F-ITA for SPI, c) IPTA for water availability, d) F-ITA for SPEI.

1951 and 2021. The second station selected was Nagymaros, situated along the Danube River in Hungary. This station was utilized to gather streamflow data and compute the SDI. Data spanning from 1893 to 2022 were utilized for this station to ensure a comprehensive representation of various climatic conditions, given Hungary's continental climate with cold winters and warm summers. The monthly average streamflow within the study period is 2326.7 m^3/s. These selected stations provide diverse climate conditions and continuous, long-term datasets necessary for a robust analysis of drought trends and their associated parameters. Table 2 summarizes the statistical information for both precipitation and temperature data for Kadıköy station and streamflow data for Nagymaros station at the Danube River.

4. Results

The P-IPTA application is carried out at five different timescales (1–3-6–9 and 12 months) for precipitation (P), water availability (WA), and streamflow data, using Kadıköy meteorology and Danube River hydrology stations as reference, and the results are obtained. All graphs and tables are presented below. This study also investigates possible drought trends for the examined stations. Firstly, P, WA, and streamflow data are fitted to the appropriate probability distribution functions, and standardized drought indices SPI, SPEI, and SDI are calculated. Monthly PET calculations are calculated using the Thornthwaite method (Thornthwaite, 1948) to determine WA values. The Kolmogorov-Smirnov test was used to determine the probability distribution functions (PDFs). The selected PDF for each dataset and time scale were summarized as follows: For precipitation, a Gamma distribution was consistently used across all time scales, including P-1, P-3, P-6, P-9, and P-12. For the water availability, the GEV distribution was applied uniformly across the time scales. For streamflow, a Gamma distribution was used for S-1, S-3, S-6, and S-9, while a Weibull distribution was selected for S-12.

4.1. IPTA for precipitation and water availability and F-ITA for SPI and SPEI at 1-month timescale

When the IPTA graph of precipitation data for rainy months in Kadıköy 1-month timescale is examined, there is a transition from an increasing trend in October to a decreasing trend in November (Fig. 4.a). While there is a significant difference in precipitation from October to November in the first period, this difference decreased in the second half period. It is seen that the increase in October precipitation and the decrease in November precipitation are effective in this way. According to Fig. 4.a, another transition trend is in Apr-May-Jun, when precipitation partially decreases. Also, while there is a slight decrease in April precipitation, there is a significant increase in June precipitation based on IPTA graph (Fig. 4.a). July-August-September and September-

Table 3
The application of the new periodic innovative polygon trend analysis P − IPTA method.

Stations		Jan.-Feb.	Feb.-Mar.	Mar.-Apr.	Apr.-May.	May.-Jun.	Jun.-Jul.	Jul.-Aug.	Aug.-Sep.	Sep.-Oct.	Oct.-Nov.	Nov.-Dec.	Dec.-Jan.
Precipitation transitional trend lengths (mm)	**1-months**	28.06	8.80	28.03	19.46	11.35	8.15	9.52	18.75	**44.73**	24.09	34.06	34.98
	3-months	60.79	56.05	54.75	33.10	4.85	23.06	67.96	80.28	**94.43**	47.01	19.35	62.11
	6-months	93.71	60.79	33.69	38.72	75.67	114.80	95.06	61.85	32.84	38.82	75.03	**115.82**
	9-months	43.44	20.71	60.74	62.36	57.13	53.74	33.07	5.25	23.10	67.82	81.14	**94.30**
	12-months	4.07	1.49	1.16	0.13	1.46	0.10	0.70	2.76	0.48	4.51	4.79	**6.83**
Precipitation transitional trend slopes	**1-months**	0.02	1.33	0.78	0.87	−0.29	**2.99**	0.25	0.61	2.53	0.28	0.49	2.78
	3-months	0.45	0.88	0.56	0.62	0.54	0.19	1.29	1.04	0.90	−0.32	**1.85**	0.81
	6-months	0.51	0.85	0.90	2.68	1.08	0.73	0.46	0.88	0.94	**2.70**	1.04	0.72
	9-months	−0.27	**1.98**	0.90	0.38	0.91	0.58	0.61	0.98	0.20	1.26	0.97	0.94
	12-months	−1.00	**12.60**	0.00	−3.42	−2.65	4.86	−1.17	−0.50	−0.65	−1.73	−1.81	−2.43
Water availability transitional trend lengths (mm)	**1-months**	32.80	22.81	58.12	72.91	62.35	42.04	21.63	79.69	89.53	57.99	53.33	28.44
	3-months	11.78	64.69	105.16	153.68	193.29	176.60	82.56	60.61	189.36	225.16	198.32	95.32
	6-months	233.41	131.42	19.22	142.60	257.91	280.40	236.09	133.73	17.88	142.68	257.97	285.29
	9-months	152.94	191.23	173.24	80.07	63.06	189.55	225.10	198.41	96.91	11.30	64.69	116.96
	12-months	3.07	0.10	0.57	2.16	2.81	4.17	4.05	2.48	1.75	1.36	3.16	11.07
Water availability transitional trend slopes	**1-months**	−0.06	1.14	0.99	0.88	0.86	1.32	0.72	0.93	1.43	0.74	0.76	243.95
	3-months	0.46	1.00	0.63	0.96	0.91	0.96	1.11	0.66	1.10	1.04	1.00	0.48
	6-months	1.04	1.06	−15.19	1.01	0.93	0.82	1.01	1.04	−185.13	0.99	0.91	0.84
	9-months	0.99	0.92	0.99	1.21	0.65	1.12	1.05	1.03	0.43	0.60	0.91	0.61
	12-months	−0.67	−97.03	0.26	−0.48	−0.01	0.14	−0.05	0.47	−1.12	−0.88	−1.05	0.76

October are other months where trend transitions are observed. There is a decreasing trend in precipitation in September, and the trend increases in October. For the Jul-Sep transition, the trend increases in July; there is no trend in August, and the trend decreases in September precipitation.

Considering the transition lengths (Table 3), which are a measure of changes in precipitation amounts and precipitation trends, it is seen that the important changes in precipitation amounts for a 1-month time scale, starting from September to April, are significant partly for the first half period and partly for the second half period, except for the Feb-Mar transition. Contrary to the precipitation change in the first half period between September and October, the precipitation change in the second period increases significantly after the decrease in September precipitation and the increasing trend in October. According to a 1-month timescale, the most significant decreasing trend in precipitation is experienced in January (Table 3 and Fig. 4.a). Despite the decreasing trend in the average precipitation of December in the second period, this month is still the month with the highest amount of precipitation. Whilst there is a small difference between the average precipitation amounts of December and January in the first half period (1953——1986), this difference increases significantly in the second half period with a significant decreasing trend in January precipitation. January, the month with the highest precipitation for the region after December, falls to fifth place after February, with a significantly decreasing trend. It can be noticed that precipitation trends decrease considerably in the winter season, that is, the November-February period, the rainiest period with November. It is determined that February precipitation also has a decreasing trend, but the decrease is much less compared to January and December. The significant difference observed between January and February precipitation in the first half period has disappeared for the second half period. As for the summer, there is a small increase in precipitation, with an increasing trend in June and July. The seasonal transitional lengths range from 8.15 to 44.73 (mm) for the precipitation, and seasonal transitional slopes range from − 0.29 to 2.99 for the 1-month timescale (Table 3).

Fig. 4.C shows the ipta graph presented for water availability (wa). wa expresses the difference between measured precipitation and calculatedpotential evapotranspiration (PET) in the study area, using a 1-month timescale as a reference. First of all, WA trends are more stable than P trends. It is determined that the trends are generally close to each other and generally decreasing, except for June, and October. While there is no trend in June, a negligible decrease (increase) is observed in May (October). The most significant decreasing trend within months is in January, as in total P. Therefore, it is seen that there is not much change in the trends for WA except in these four months, and the calculated seasonal transition lengths and slopes are more stable compared to precipitation (Table 3).

As seen in Fig. 4.b and Fig. 4.d, there are cases where the dry and wet periods at the same station do not match. Similarly, it is seen that the frequency and classification of drought events vary depending on the indices. As previously mentioned in the methodology section, the F-ITA method is used to reveal trends in drought events defined according to

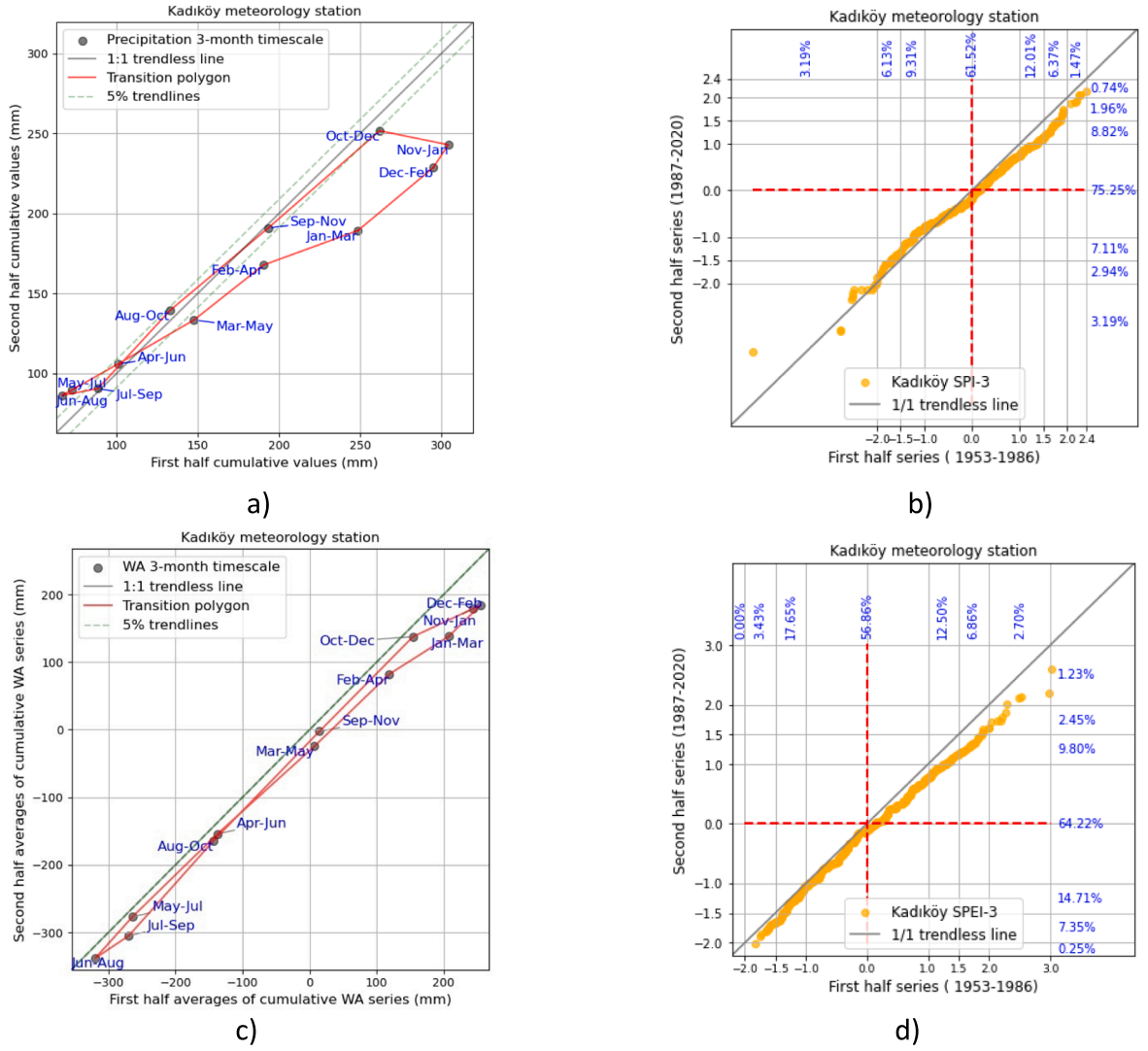

Fig. 5. P-IPTA and F-ITA graphs for Kadıköy station at a 3-month timescale. a) P-IPTA for precipitation, b) F-ITA for SPI, c) P-IPTA for water availability, d) F-ITA for SPEI.

drought indices. In addition, by adding F-ITA graphs (Fig. 4.b and Fig. 4.d), which contain the frequency values of each drought classification, trends and possible frequencies and changes according to two different periods, could be defined for each drought classification in this research.

For Kadıköy meteorological station, the trends of defined drought classifications for time series and timescales, considering the SPI and SPEI indices, are given in Fig. 4.b and Fig. 4.d, with the graphical interpretation of F-ITA. Monotonic and non-monotonic increase–decrease trends are determined according to drought and wet classifications. According to the SPI-1 and SPEI-1F-ITA graphs (Fig. 4.b and Fig. 4.d), the wet classification has a monotonic decreasing trend regarding the 0–0 coordinate system. The SPEI-1F-ITA graph shows that the determined wet classifications tend to decrease monotonically. When SPI-1 and SPEI-1F-ITA graphs are compared in terms of wet periods, it can be stated that the monotonic decreasing trend in SPEI indices in the 1987–2020 period is more evident than SPI. Also, trends are examined one by one for each drought classification in Table 1 for both SPI and SPEI. While the SPI index values for the MW classification decrease slightly in the second period, it is clear that in terms of the frequency of the drought classifications, the number of events falling in the first (12.5 %) and second period (11.03 %) is very similar and no obvious trend can be observed (Fig. 4.b). There is a significant monotonic decreasing trend for SW and EW classifications. The frequencies, which are 5.88 % and 1.96 %, respectively, for the SW and EW in the 1951–1986 period (first period), are decreased to 3.92 % and 0.98 % in the 1987–2020 period (second period).

For SPEI-1F-ITA graph (Fig. 4.d), the frequencies of MW, SW, and EW classifications decrease significantly in the second period compared to the first period, with a decrease in the trends in drought index values. In the period 1953–1986, the frequencies for $1.0 \leq$ SPI-1 (SPEI-1) <1.5 (MW), $1.5 \leq$ SPEI-1 <2.0 (SW) and SPEI-1 ≥ 2.0 (EW) classifications are 12.5 %, 4.66 % and 1.72 %, respectively, and they decrease slightly in the 1987–2020 period and is calculated as 8.82 %, 3.43 %, and 0.74 %. When the comments given above for the IPTA graph for a one-month timescale are examined, the reasons for the trends and changes generally seen in wet events from October to March are better understood.

The SPI-1 (SPEI-1) trends at MD, SD, and ED classifications are also examined in detail with F-ITA graph. For SPI-1 calculated for the MD classification, the frequencies of this classification in both periods are very close. SPI values in the SD classification between 1953 and 1986 show a slight tendency to decrease towards the MD classification in the second half period. When the frequencies calculated for the SD classification of the first (5.39 %) and second period (5.64 %) are examined, it is seen that there is no significant change between the two periods. For SPEI-1 calculations, the most important difference is seen in the ED classification compared to SPI calculations. According to SPEI-1 (Fig. 4.

d), while ED events do not occur in any month in the 1953–1986 period, the frequency of ED events in 1987–2020 is limited to only 0.98 %. On the other hand, according to Fig. 4.b, the frequencies of ED events for SPI-1 in the first and second half periods are 6.62 % and 4.90 %, respectively. Based on the SPEI-1F-ITA graph (Fig. 4.d), the trend direction shows a monotonic increase for the MD and SD classifications. Depending on this trend direction, the frequency changes in the relevant drought classifications for SPI-1 (SPEI-1) decrease from 8.09 % (12.25 %) to 7.84 % (10.54 %) in 1953–1986 for MD classification, while the SD classification for both SPI-1 and SPEI-1 increases from 5.39 % (6.86 %) to 5.64 % (8.58 %).

4.2. P – IPTA for precipitation and water availability and F-ITA for SPI and SPEI at a 3-month timescale

Fig. 4.a and c show cumulative precipitation (CP) and water availability (WA) data trends. For this purpose, the P-IPTA graphs are recommended within the scope of the study. For a 3-month period, when the first and second halves are evaluated together according to the P-IPTA graphs, it can be noticed that the rainiest periods are between October – February period, and the period with the least precipitation is between May – September period (Fig. 5.a). For P-IPTA trend graphs presented for three-month WA, the water surplus is highest in the Nov-Feb period in the first half, while the Jun-Aug period is the most critical in terms of water deficit (Fig. 5.c). According to the first half period covering the years 1951–1985, the rainiest three-month period is the Nov-Jan period, followed by the Dec-Feb period. Looking at the years 1986–2020, it can be seen that the rainiest period changed to Oct-Dec. The main reason for the change in the periods with the highest precipitation is the significant decrease in precipitation, especially in the Nov-Feb period. While precipitation tends to decrease in precipitation in the Oct-Dec period, this decrease is limited compared to the Nov-Jan and Dec-Feb periods. The decreasing trends in autumn, spring, and especially winter precipitation for three-month periods are striking. On the other hand, precipitation is increasing during the May-Jul and Jun-Aug periods, which include the summer months. For the months of Jul-Sep, Apr-Jun, Aug-Oct, and Sep-Nov, it is seen that the distributions of the calculated trends are close to the 1:1 trendless line within 5 % trendlines, and it can be said that there is no trend.

The trends in P-IPTA WA graphs presented for the three-month time scale decrease within the twelve periods considered (Fig. 5.c). The largest decreasing trend for water availability occurs in the Nov-Jan, Dec-Feb, and Jan-Mar periods. On the other hand, the most significant decreasing trends for WA are in the Jul-Sep and Jun-Aug periods. Compared to the P-IPTA CP graphs, the three-month P-IPTA WA graphs indicate more stable trends in the twelve periods considered and in the

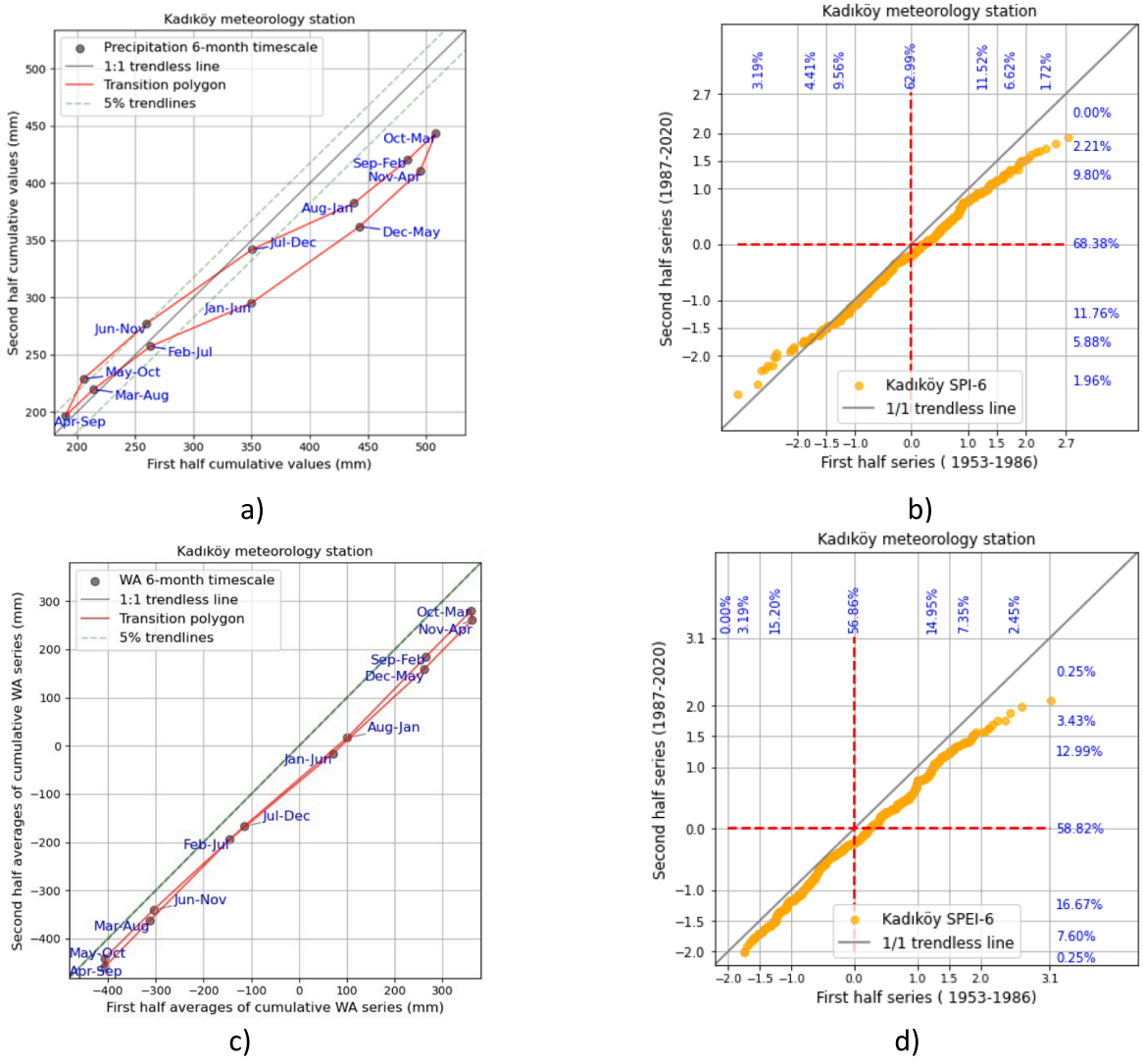

Fig. 6. P-IPTA and F-ITA graphs for Kadıköy station at a 6-month timescale. a) P-IPTA for precipitation, b) F-ITA for SPI, c) P-IPTA for water availability, d) F-ITA for SPEI.

transitions between periods (Table 3). As for SPI-3 and SPEI-3 results calculated using the time series of CP and WA amounts (Fig. 5.a and c), a non-monotonic decreasing trend can be noticed when the F-ITA graphic results are evaluated as a whole only for the dry and wet periods without considering the sub-classification intervals.

When the trends and frequency changes are evaluated according to the drought classifications defined based on SPI theory by Mc Kee et al. (1993), for EW and SW classifications, the trend decreases slightly according to the calculated SPI-3 and SPEI-3 values. Also, it is understood that the trend is slightly decreasing, and the probability of EW and SW events has increased significantly in the second period compared to the first period. Considering the F-ITA graphs (Fig. 5.b and d) and frequency values for the MW classification for SPI-3 (SPEI-3), a significant decreasing trend is observed, the total number of drought events occurring in the second 8.82 % (9.80 %) and first periods 12.01 % (12.50 %) in this classification. It is seen that the rate (frequency) within it changes significantly.

According to the F-ITA SPI-3 and SPEI-3 (Fig. 5.b and d), when the trends for drought classifications with negative index values and the frequencies of each drought classification in the determined periods are examined, there is no significant trend for the ED classification, and the frequency of drought events no or very little change in the two periods. SD classification for SPI-3 (SPEI-3) shows a decreasing (increasing) trend. Also, the incidence of relevant drought events in the years 1953–1986 change from 6.13 % (3.43 %) to 2.94 % (7.35 %) compared to the second period. Finally, for MD classification, the SPI-3 (SPEI-3) trend decreases (increases) based on the drought index, and the frequencies of MD events decrease from 9.31 % (17.65 %) to 7.11 % (14.71 %) over time. Briefly, when the F-ITA SPI-3 graph is examined, after the non-monotonic decreasing trend in drought and wet events seen in the Kadıköy region, the normal classification range of 1.0 > SPI-3 $\geq$ -1.0 in the 1987–2020 period increases from 61.52 % to 75.25 %. According to the F-ITA SPEI-3 analysis results, the increasing trend in drought events occurs significantly between SD and MD. In contrast, the decreasing trend in wet events affects all classifications. Therefore, the event frequencies in the normal classification increase from 56.86 % in the first period to 64.22 % in the second period.

4.3. P – IPTA for precipitation and water availability and F-ITA for SPI and SPEI at a 6-month timescale

For P-IPTA graphs for both CP and CWA at 6-month timescales, the polygon geometries in which trends and trend transitions are defined differ significantly compared to the geometries of 1 and 3-month time scales, and the trends between successive periods approach each other (Fig. 6.a and c). When the meaning and main reason for this difference

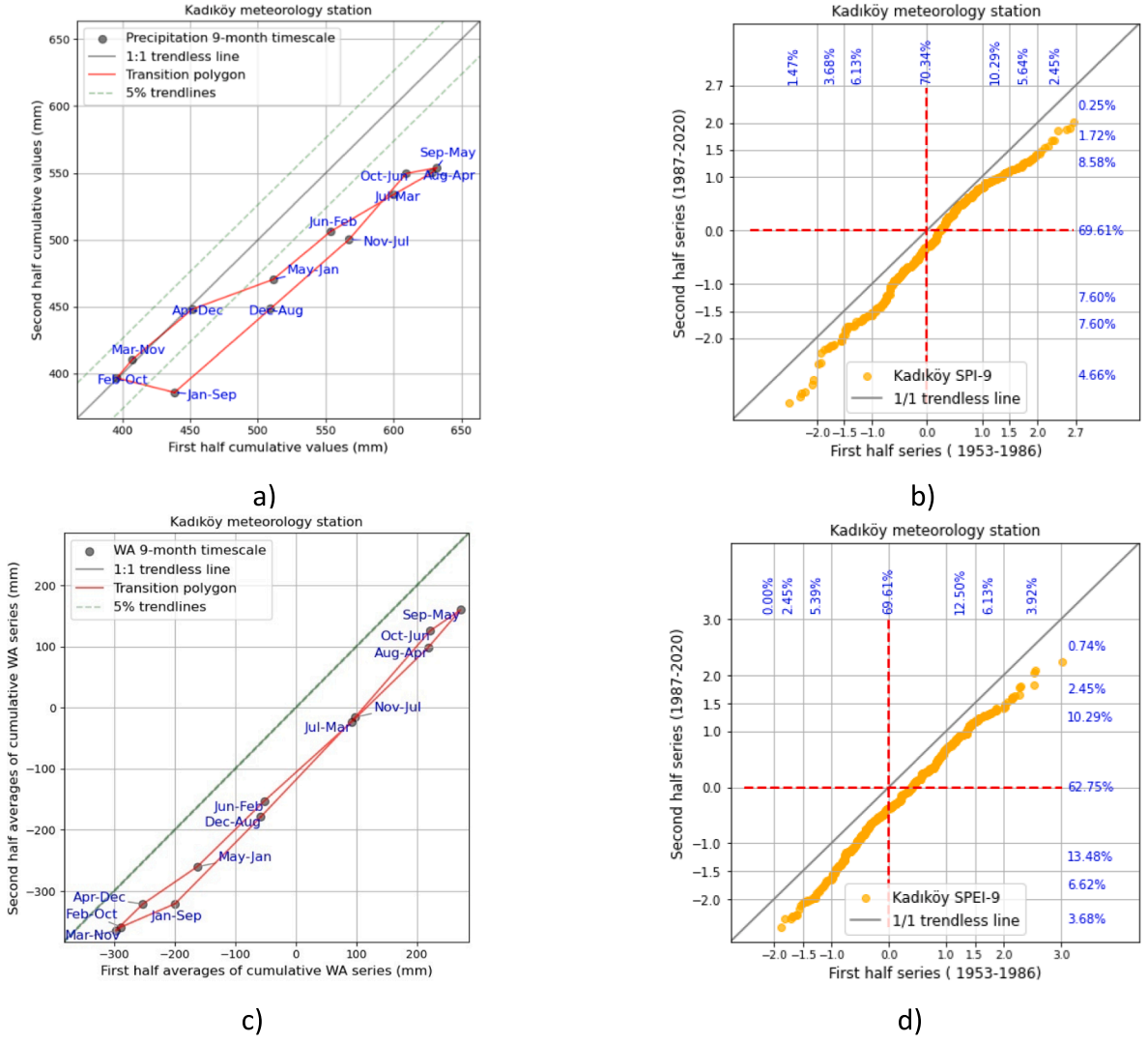

Fig. 7. P-IPTA and F-ITA graphs for Kadıköy station at a 9-month timescale. a) P-IPTA for precipitation, b) F-ITA for SPI, c) P-IPTA for water availability, d) F-ITA for SPEI.

are investigated, it is seen that the trend direction becomes more evident as timescales increase. For the P-IPTA graph for CP-6, it is seen that especially the rainy periods tend to decrease and, for CP-6 > 350 mm, the precipitation amounts in the Aug-Jan, Sep-Feb, Oct-Mar, Nov-Apr, and Dec-May periods increase as period transitions and trend magnitudes approach each other (Table 3). For example, P-IPTA graphs presented for the 1 and 3-month time scale in Fig. 4.a and Fig. 5.a are compared, it is seen that for the 1-month time scale, the transition lengths between Dec, Jan, and Feb, when the greatest precipitation is seen, are Oct-Dec, Nov-Jan, for the most important precipitations in the 3-month period. It is seen that the transition lengths between the Nov-Jan and Dec-Feb periods are decreasing, and the trend points are relatively approaching each other (Table 3). The relative decrease in the distances between trend points and the shortening of transition lengths make the trend direction clear. Similarly, when the 3- and 6-month graphs are compared for the rainiest periods, the total precipitation amounts and trends of the 6-month Sep-Feb, Oct-Mar, and Nov-Apr periods are closer to each other compared to the 3-month Oct-Dec, Nov-Jan, and Dec-Feb periods (Fig. 5.a and Fig. 6.a).

Fig. 6.C shows the water surplus and water deficit p-ipta graphs at six-month timescales. according to the wa evaluation, there are seven wet periods for precipitation starting from the jul-dec period and lasting until the jan-jun period, and twelve, where the pet effect is considered. the trends are decreasing throughout the period, as seen in Fig. 6.c and Table 3. Also, the trend sizes are close to each other, especially for WA. For CP-6, there is no trend in the Feb-Jul, March-Aug, and Apr-Sep periods within 5% trendlines, and the trends increase in May-Oct and Jun-Nov. Additionally, F-ITA – SPI-6/SPEI-6 graphs (Fig. 6.b and d) presented for CP and CWA show that both graphic trends are decreasing for the wet classifications and increasing trend for the drought classifications. For EW and SW classifications and according to the first half (1953 – 1986), SPI-6 decreases from 1.72% and 6.62% to 0% and 2.21%, respectively. SPEI-6 decreases from 2.45% and 7.35% to 0.25% and 3.43%, respectively. Considering the F-ITA – SPI-6 (SPEI-6) graphs for the MW classification, a decreasing trend is seen, and the frequencies accordingly decrease slightly from 11.52% (14.95%) to 9.80% (12.99%), respectively.

On the other hand, the frequency of ED classification for SPI-6 decreases from 3.19 % to 1.96 %. For SPEI-6, while there are no ED events in this classification in the 1953–1986 half, a small amount of ED events are detected in the 1987–2020 half, and its frequency is determined as 0.25 %. According to F-ITA graphs for both SPI-6 and SPEI-6, a non-monotonic decreasing trend in SD classification is seen for SPI-6, while there is a significant increase in this classification compared to SPEI-6. For F-ITA SPI-6 and SD classification, the frequency increases from 4.41 % in the 1953–1986 half to 5.88 % in the 1987–2020 half, and

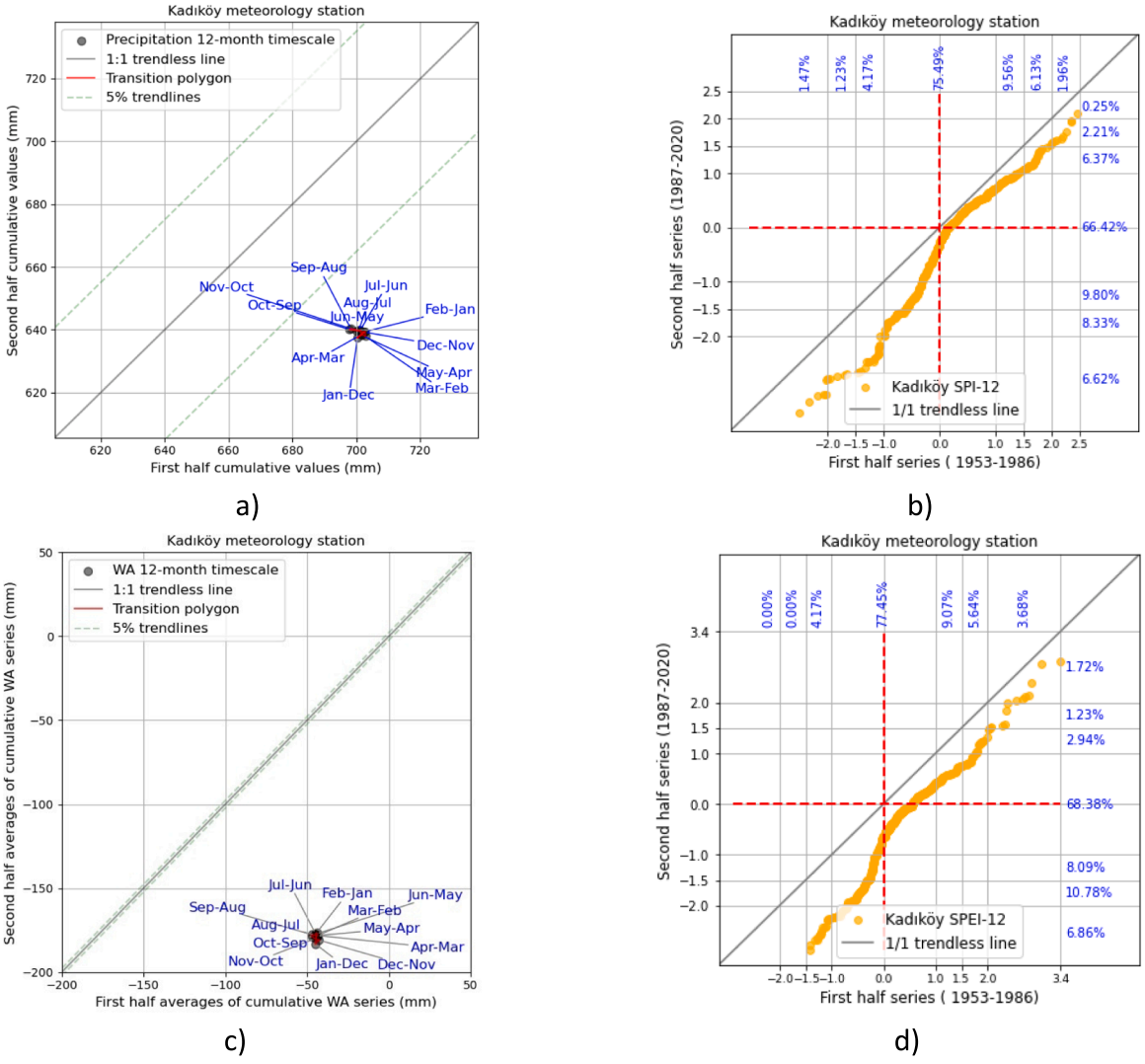

Fig. 8. P-IPTA and F-ITA graphs for Kadıköy station at a 12-month timescale. a) P-IPTA for precipitation, b) F-ITA for SPI, c) P-IPTA for water availability, d) F-ITA for SPEI.

for F-ITA SPEI-6 and SD classification, the frequency increases from 3.19 % to 7.60 %. Finally, according to the SPI-6 and SPEI-6 results, SPI-6 (SPEI-6) F-ITA graphs for the MD classification, there is an increasing trend in their frequencies from 9.56 % (15.20 %) to 11.76 % (16.67 %), respectively.

4.4. *P − IPTA for precipitation and water availability and F-ITA for SPI and SPEI at a 9-month timescale*

For CP-9/CWA-9P-IPTA graphs (Fig. 7. a and c), the CP generally tends to decrease significantly, and total precipitation differences between periods decrease. According to Fig. 7. a, three of the twelve different periods, Feb-Oct, Mar-Nov, and Apr-Dec, have no trend. Accordingly, when the SPI-9F-ITA graph is interpreted (Fig. 7.b), it can be stated that the SPI-9 values in the first quadrant area in the Cartesian coordinate system, where SPI-9 values are positive, tend to decrease significantly monotonically. On the contrary, SPI-9 values in the third quarter area show a significant increasing trend. As a result of the significant decrease in the trends in all periods determined by the WA P-IPTA graph (Fig. 7.c), as can be seen from the SPEI-9F-ITA graph (Fig. 7. d), water surplus events decrease significantly, while significant increasing trends exist in water deficit events.

Based on the drought and wet classifications and for the normal classification values ranging between 1.0 and −1.0, wet classification generally decreases, while drought indices at drought classification tend to increase slightly for both SPI-9 and SPEI-9 (Fig. 7.b and d). Accordingly, the frequencies of events in the normal classification for SPI-9 (SPEI-9) indices decrease from 70.34 % (69.61 %) in 1953–1986 to 69.61 % (62.75 %) in 1987–2020. Based on a detailed evaluation of the trends and frequencies of drought events regarding each drought

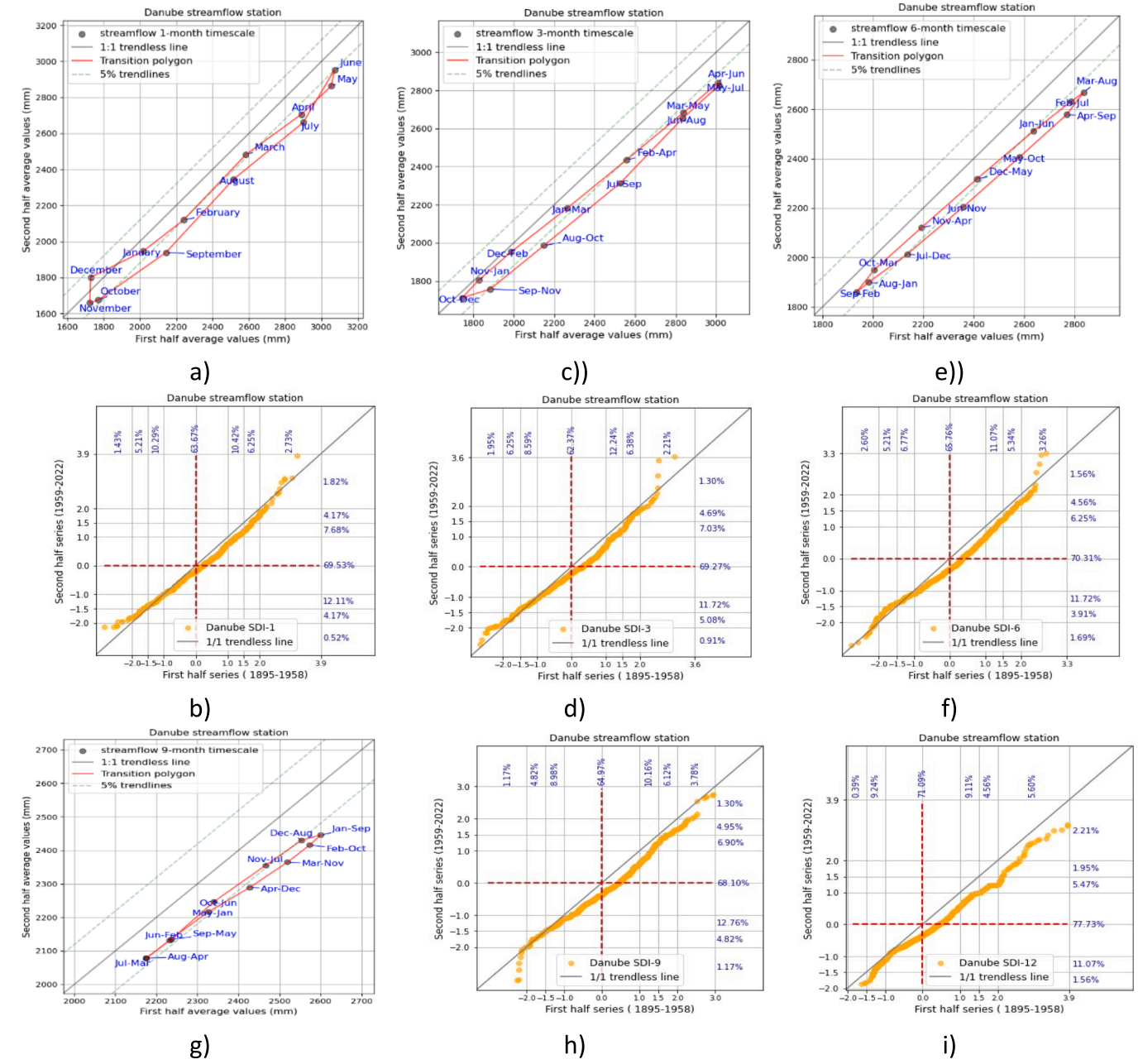

Fig. 9. The applications of the P-IPTA methods for Danube Streamflow and SDI series. a) P-PTA for streamflow data at 1-month, b) F-ITA for SDI-1, c) P-PTA for streamflow at 3-month d) F-ITA for SDI-3, e) P-PTA for streamflow at 6-month, f) F-ITA for SDI-6, g) P-PTA for streamflow at 9-month, h) F-ITA for SDI-9, i) F-ITA for SDI-12.

classification for F-ITA SPI-9 (SPEI-9), there is a significant trend towards an increase for the ED category, and in the second period, the frequency of drought events increases from 1.47 % (0 %) to 4.66 % (3.68 %). Similarly, there is a significant increasing trend according to the SPI-9 (SPEI-9) index values calculated for the SD classification, and the frequency of drought events increases significantly in the last period compared to the first period, from 3.68 % (2.45 %) to 7.60 % (6.62 %).

Finally, MD for SPI-9 (SPEI-9) is insignificant (significant) in terms of drought event frequencies between two periods, from 6.13 % (5.39 %) in 1953–1986 to 7.60 % (13.48 %) in the 1987–2020 period. Also, the trend is towards a significant decrease according to the calculated SPI (SPEI) index values for EW and SW. In the first half, the EW and SW frequencies for SPI-9 (SPEI-9) decrease from 2.45 % – 5.64 % (3.92 % – 6.13 %) to 0.25 % – 1.72 % (0.74 % – 2.45 %) in the second period, respectively (Fig. 7.b and d).

4.5. P – IPTA results for precipitation and water availability and F-ITA results for SPI and SPEI at a 12-month timescale

For P-IPTA graphs CP-12 (WA-12) for a full twelve-month period (Fig. 8.a and c), the CP and WA deficit are clustered around a certain point and tend to decrease significantly without any specific polygon. According to the F-ITA graphs in (Fig. 8.b and d) below, while SPI-12 (SPEI-12) patterns have a very obvious monotonic increasing trend for drought, wet events have the opposite monotonic decreasing trend. These results show that the region has become drier over time. When the trends and frequencies for all drought classifications starting from EW to ED are evaluated with reference to F-ITA SPI-12 and F-ITA SPEI-12 graphs, it is clearly seen that there is a significant decreasing (increasing) trend for wet (drought). According to (SPEI-12) and EW, SW, and MW drought classifications, the trends are decreasing. Also, the frequencies are respectively 1.96 % (3.68 %), 6.13 % (5.64 %), 9.56 % (9.07 %) in the first half, and 0.25 % (1.72 %), 2.21 % (1.23 %), and 6.37 % (2.94 %) in the second half. The trend results for SPI-12 and SPEI-12 indices for drought events differ further. First of all, when evaluating the ED classification, the trend for SPI-12 (SPEI-12) is increasing, and its frequency varies from 1.47 % (0 %) to 6.62 % (6.86). Also, according to the F-ITA SPI-12 (SPEI-12) graphs for SD classification (Fig. 8.b and d), graphs show a monotonic increase, while the relevant classification in both graphs increases from 1.23 % (0)% in the first half to 8.33 % (10.78 %) in the second half.

4.6. P – IPTA results for streamflow (R) data and F-ITA results for SDI

Considering the monthly average streamflow data measured at the Danube River station between 1895 and 2022, the trends of the river's streamflow data for 1–3-6–9 and 12-month timescales are determined with the help of the P-IPTA method proposed in this research (Fig. 9). The region is evaluated regarding hydrological drought, considering the SDI index calculated with reference to different timescales mentioned above. The trends of the SDI time series are defined using the F-ITA method. As a result of the analyses, the increasing and decreasing trends in the drought time series and the periods whether there is any trend were determined (Fig. 9).

For the P-IPTA graph for R, the dominant negative trends prevail in almost every period. For a one-month timescale (Fig. 9.a), the trend little increases only in December within the 5 % treandlines, when streamflows in the river are low. In other months, there has been a decreasing trend in streamflows of around 5 % or more. It is understood that the decreasing tendencies are above 5 %, especially in periods when the streamflows are above the annual averages.

This makes the region even more dry in terms of wetlands. When F-ITA SDI-1 graph is examined (Fig. 9.b), the trend in terms of wetness is clearly decreasing. Also, for wet periods, the frequencies of the 1895–1958 period for the EW, SW, and MW classifications are 2.73 %, 6.25 %, and 10.42 %, respectively. It is understood that the frequencies decreased to 1.82 %, 4.17 %, and 7.68 %, respectively, in the 1959–2022 period. For drought classifications, there is a decreasing trend only in the ED classification, and there is no trend in the SD and MD classifications. As can be seen from the F-ITA SDI-1 graph, the frequencies of these classifications have also changed slightly.

4.7. Classical and proposed trend analysis results

To compare the P-IPTA and F-ITA with conventional Mann-Kendall (MK), Sen's slope estimator (SSE), and innovative Şen's trend analysis (Şen's ITA) methods, we have designed Table 4. As seen from the table, all parameters of the employed trend analysis methods are negative, and the absolute parameters values increase with the durations of the periods. This finding is consistent with the World Meteorological Organization's definition of drought: "Drought is a prolonged dry period in the natural climate cycle that can occur anywhere in the world". Although the MK does not indicate a decreasing trend on the 1-months cumulative precipitation series at the 90 % significance level ($z_{MK} \geq |1.65|$), it does show decreasing trends in the 3-months, 6-months, 9-months, and 12-months cumulative precipitation series. Unlike Şen's ITA, the Mann-Kendall (MK) and Sen's slope estimator (SSE) methods provide decisions on monotonic trends and slopes. The innovative polygon trend analysis (IPTA) method, developed by Şen's ITA, enables the inspection of seasonal trends in time series by dividing seasonal data ranges into various groups, such as low, medium, and high values. Additionally, the frequency innovative trend analysis (F-ITA) allows examinations of changes in the frequencies of subgroups (low, medium, and high) within time series. This approach addresses the distortion of hydrometeorological series probability density functions, referred to as non-stationary conditions, resulting from climate changes (Milly et al. 2008; Alashan 2018, 2024).

4.8. Innovative monthly trend chart results

Fig. 10 below shows the innovative monthly trend chart for precipitation, water availability, and streamflow records at 1-month and 6-month timescales. The trend at each month is calculated using P-IPTA method. In general, there appears to be a decreasing trend across all

Table 4
Classical trend analysis parameters and slopes of the Mann-Kendall, Sen's Slope estimator, and Şen's innovative trend analysis methods.

Stations	Variables	Trend parameters	Time scale				
			1-months	3-months	6-months	9-months	12-months
Kadıköy	Cumulative Precipitation (mm)	Z_{MK}	−0.983	−1.926	−3.005	−4.143	−4.613
		S_{SSE}	−0.005	−0.027	−0.063	−0.088	−0.102
		S_{ITA}	−0.012	−0.036	−0.072	−0.108	−0.146
	Water Availability (mm)	Z_{MK}	−2.250	−2.900	−3.901	−6.678	−12.107
		S_{SSE}	−0.028	−0.091	−0.172	−0.252	−0.298
		S_{ITA}	−0.028	−0.081	−0.161	−0.247	−0.333
Danube	Streamflow (m^3/s)	Z_{MK}	−3.124	−3.850	−5.071	−6.312	−6.939
		S_{SSE}	−0.149	−0.478	−0.097	−1.420	−1.794
		S_{ITA}	−0.174	−0.522	−1.036	−1.519	−1.965

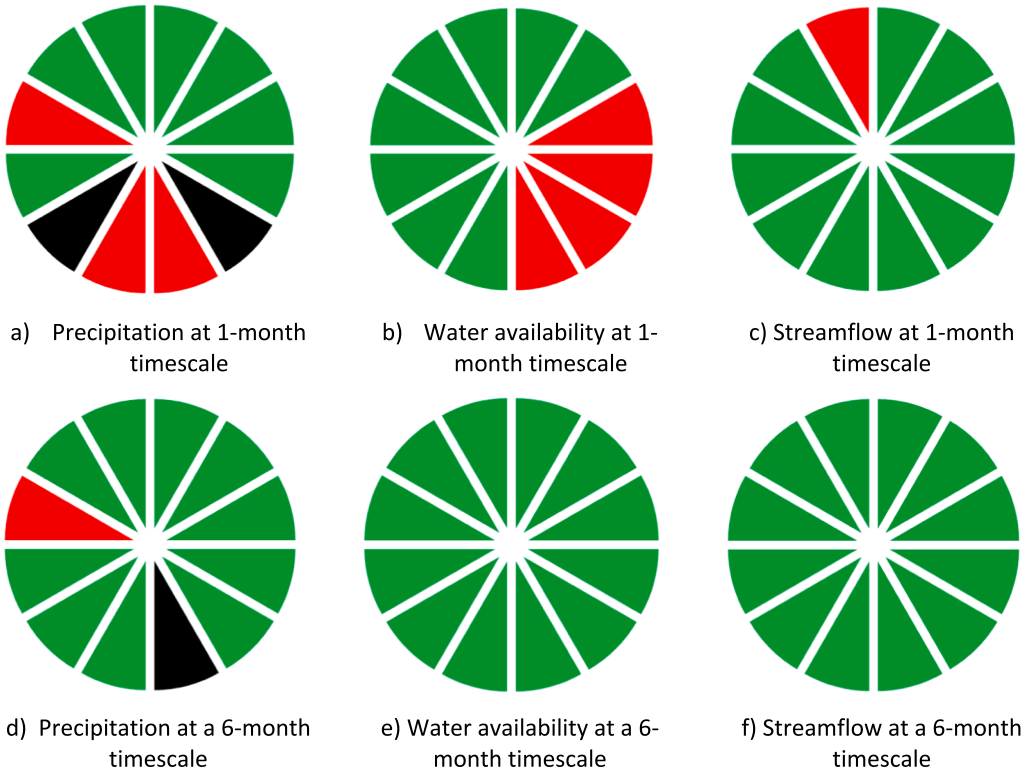

Fig. 10. Innovative Monthly Trend Chart for different hydro-meteorological variables and timescales.

variables examined. For instance, when considering the monthly trends for WA and R at a 6-month timescale, both exhibit a decreasing trend in all months. However, it is noteworthy that while the WA trend at a 1-month timescale demonstrates an overall decreasing trend, there are increasing trends observed in March, April, May, and June. This figure allows for a comparative analysis of trends across different variables and timescales, facilitating a comprehensive understanding of the changing trends.

5. Discussion

The analysis conducted using the newly proposed P-IPTA method revealed generally a consistent decreasing trend in precipitation across various timescales (Figs. 4-8). For instance, at a 1-month timescale, the original IPTA method, the monthly average precipitation for January decreased from approximately 105 mm in the first half to 63 mm in the second half. This declining trend becomes more pronounced over longer timescales, such as 9 months. These findings are consistent with previous research by Kömüşcü and Aksoy (2023), who reported similar trends in precipitation. Specifically, they noted predominant decreases in precipitation during the wet season, with increasing trends observed in the dry season. Monotonic trends on a monthly basis indicated larger downward trends, particularly during early winter and spring. Additionally, Nacar et al. (2024), in their investigation of historical and future scenarios for precipitation trends in the western Black Sea region, also observed a declining trend, underscoring the importance of comprehensive studies on precipitation trends and drought assessment. Körük et al. (2023) highlighted the effectiveness of ITA and IPTA methods for trend identification compared to classical approaches. This trend is evident in this research examining droughts and their associated parameters.

In terms of water availability, as proposed by Vicente-Serrano et al. (2010), the number of articles addressing the trend of water availability is limited. For instance, in Türkiye, only Dadaser-Celik et al. (2016) researched evapotranspiration trends, with the results indicating a decreasing trend. Subsequently, analyzing the trend of one-month and cumulative water availability is crucial for effective water resources management and drought studies. This study revealed decreasing trends across all months and timescales, with each exhibiting a consistent magnitude of decrease. Notably, the polygon formed by these trends was parallel to the 1:1 line, indicating the same trend magnitude. These findings underscore the urgency for decision-makers to take appropriate actions in response to the significant decreasing trend observed in water availability.

Numerous studies have been conducted in the literature regarding SPEI at different timescales. For instance, Danandeh Mehr and Vaheddoost (2020) calculated the trend of SPEI at 3, 6, and 12-month timescales for Ankara province in Türkiye, revealing slight decreasing trends. Similarly, Serkendiz et al. (2024) analyzed the trend of SPEI across Türkiye from 1970 to 2019, identifying a gradual north-to-south increase in drought intensity. Their study did not consider the trend in water availability, leading to not comprehensively understanding the relationship between SPEI trends and actual water availability. In our research, the SPEI results indicated an increasing trend in drought index (SPEI less than −1), along with decreasing trends for normal and wet events (SPEI more than −1), aligning with previous study findings.

In the existing literature, articles focusing on hydrological drought based on streamflow data are scarce compared to those addressing meteorological drought using SPI and SPEI. Moreover, while some studies have calculated hydrological drought indices and analyzed trends in streamflow data, they often do not explore the relationship between the trend of the hydrological drought index and the original streamflow data (Katipoğlu and Acar 2022; Yuce et al. 2023). This research aims to bridge this gap by investigating the relationship between hydrological drought trends and streamflow data trends. For instance, the P-IPTA graphs for streamflow data in this study reveal a decreasing trend across all timescales (Fig. 9). This unexpected finding prompts further exploration into the underlying factors influencing drought trends. In their study, Katipoğlu and Acar (2022) determined decreasing trends in about 60 % of the stations. Additionally, the

analysis of SDI trends based on F-ITA for a 12-month timescale shows a decreasing trend in drought (Fig. 9), which may be attributed to various factors, including the assumption used for calculating streamflow trends and the selected probability distribution function for fitting the original data. However, for normal and wet events (SDI greater than −1), the trend results for both SDI and original streamflow data are more consistent. In Yuce et al.'s (2023) study, the F-ITA method was also used for 1, 3, 6, 9, and 12-month timescales. The results were inconsistent and changed for each station. Some stations showed a decreasing trend, and some showed an increasing trend. Subsequently, one of the main contributions and key findings of this research is the recognition that both hydrological drought trends and hydrological drought-associated parameters must be carefully considered in trend and climate change studies.

Understanding water dynamics, including water availability, is crucial in terms of the context of hydrology. Water availability explains the equilibrium between water inputs and outputs, facilitating assessments of water resource availability and distribution. By quantifying components like precipitation, water availability, and streamflow and their trends, hydrologists, researchers, and decision-makers gain insights into water stress, surplus, and sustainability. Similarly, water availability determines the accessible water for various sectors, incorporating factors like precipitation patterns, stream flows, and human demands.

The suggestion of the P-IPTA method represents an enhancement of IPTA by incorporating periodic variations into trend analysis. While IPTA focuses only on evaluating temporal trends in hydrometeorological parameters across one month, P-IPTA enhances IPTA method by considering the periodic variations, offering a more comprehensive understanding of trends. On the other hand, F-ITA method incorporates the frequencies of drought classifications into trend analysis. This enables a more comprehensive assessment and evaluation of trends in meteorological and hydrological drought across different timescales. Therefore, P-IPTA and F-ITA represent significant advancements in meteo-hydrological and drought trend analysis, providing researchers with powerful tools.

One of the main contributions of this research is also the innovative monthly trend chart. Existing literature primarily focuses on trend maps based on specific months, such as those generated by IPTA method, typically produced for individual months. For instance, Katipoğlu and Acar (2022) created a trend map for each month for the Euphrates Basin in Türkiye. In contrast, this study's innovative monthly trend chart offers a distinct advantage by presenting the trend identification for all months across all stations on a single map. This approach facilitates a comprehensive assessment of trends across different timescales (Fig. 10) and geographical locations, providing valuable insights into climate change impacts' temporal and spatial variability. This chart is a valuable tool for climate change studies, enabling researchers to gain a deeper understanding of temporal trends, thereby enhancing the management of climate-related risks.

Several key differences exist between classical and innovative trend analysis methods. Traditional methods, such as Mann-Kendall and Sen's slope, often rely on assumptions of normality and serial independence alongside large sample sizes, which may limit their applicability and robustness in practical uses. Conversely, the IPTA and Şen's ITA methods do not necessitate such assumptions, employing a non-parametric approach without serial correlation and sample size restrictions. The ITA method offers enhanced flexibility in trend analysis by utilizing a scatter plot comparison on a Cartesian coordinate system, providing a more adaptable framework for analyzing hydro-meteorological time series data. Furthermore, while classical methods may be susceptible to biases from positive autocorrelation in the data or the loss of trend information due to prewhitening techniques, the ITA method aims to minimize these biases. The method's effectiveness has been demonstrated through validation using synthetic and original datasets, confirming its applicability across a wide range of hydro-meteorological variables (Şen 2017). This comparison underscores the advantages of innovative trend analysis approaches over traditional methods, emphasizing the importance of adopting more flexible and robust methodologies in hydrological research and decision-making processes.

Analyzing and assessing meteorological and hydrological droughts at various timescales and identifying their associated parameters is paramount in climate change studies, adaptation and mitigation plans, and water resources management. Understanding the relationship between drought and its associated parameters with trends is crucial for predicting their impact on ecosystems, agriculture, and other sectors. By studying droughts at different timescales, from short-term droughts to long-term droughts, researchers and decision-makers can gain insights into the complex interactions between climatic variables and water resources. This knowledge is essential for developing effective strategies to mitigate the adverse effects of drought, such as implementing water conservation measures, improving irrigation practices, and enhancing drought resilience in vulnerable regions.

6. Conclusion

Due to the effects of climate change, the importance of the trend of meteorological and hydrological droughts and their associated parameters, and the existing gap regarding the relationship between their trends, this research aimed to develop a new concept and suggest innovative trend analysis methods. Firstly, the P-IPTA method was proposed to cover the periodic variations in the hydrometeorological variables within various time scales. Then, F-ITA was suggested and applied to meteorological droughts, including SPI and SPEI, and hydrological droughts, including SDI. F-ITA has the power to incorporate the frequencies of each drought classification in the trend analysis. Also, the relationship between drought trends and associated parameter trends has been revealed. Finally, a comprehensive comparison between classical and innovative trend methods has been conducted. These comprehensive approaches allow us to examine drought dynamics and trends across various time scales, providing valuable insights into droughts and their associated parameters. This research used two applications: the first is Kadıköy station (1951—2021) for the trends of SPI and SPEI with their associated parameters, and the second is Danube River (1893—2022) for the trend of SDI and its associated parameters. The key findings and future advantages of this research can be summarized as follows:

- Understanding the relationship between the trends of droughts and their associated parameters is crucial for advancing drought and climate change studies.
- The meteorological drought assessment using SPI and SPEI and the F-ITA method reveals a decreasing trend in normal and wet classifications across all timescales, emphasizing the decreasing trends observed in precipitation and water availability datasets at Kadıköy station.
- The decreasing trends in precipitation and water availability for the Kadıköy station resulted in increasing trends in drought events across all drought classifications (MD, SD, and ED), except for SPI at 1-month and 6-month timescales, which exhibit specific drought patterns.
- SDI and streamflow trends for the Danube River showed a consistent relationship between streamflow data and normal and wet events, and the important results are partially inconsistent regarding drought events.
- The innovative trend analysis methods, including IPTA, F-ITA, and the newly proposed P-IPTA method, enable more accurate and comprehensive trend analysis for drought at different time scales.
- Utilizing the F-ITA method allows for incorporating the frequencies of drought classifications, leading to a more precise assessment. For

instance, with SPEI at a 6-month timescale, the frequency of the SD classification increased from 3.19 % to 7.6 %.

- The innovative monthly trend chart clearly shows trend changes across all months or cumulative periods and for all stations within the study area or region, indicating a decreasing trend, increasing trend, or no trend for each month or cumulative timescale and different timescales.

CRediT authorship contribution statement

Ahmad Abu Arra: Writing – review & editing, Writing – original draft, Visualization, Methodology, Formal analysis, Conceptualization. **Sadık Alashan:** Writing – review & editing, Writing – original draft, Visualization, Validation, Supervision, Methodology, Investigation, Formal analysis, Conceptualization. **Eyüp Şişman:** Writing – review & editing, Writing – original draft, Supervision, Methodology, Data curation, Conceptualization.

Declaration of competing interest

The authors declare that they have no known competing financial interests or personal relationships that could have appeared to influence the work reported in this paper.

Data availability

Data will be made available on request.

The data are available from the corresponding author upon reasonable request.

Acknowledgment

The authors would like to thank the Republic of Türkiye and the Turkish State of Meteorological Service for their support and for providing the dataset. The authors would like to acknowledge that this paper is submitted in partial fulfillment of the requirements for the PhD degree at Yildiz Technical University. This research did not receive any specific grant from funding agencies in the public, commercial, or not-for-profit sectors.

References

Abu Arra A & Şişman E)2023. (Characteristics of hydrological and meteorological drought based on intensity-duration-frequency (IDF) curves. Water 15, no. 17: 3142. doi: 10.3390/w15173142.

Abu Arra, A., Şişman, E., 2024. Innovative drought classification matrix and acceptable time period for temporal drought evaluation. Water Resour. Manag. 1–23 https://doi.org/10.1007/s11269-024-03793-0.

Alashan, S., 2018. Data analysis in nonstationary state. Water Resour Manag. https://doi.org/10.1007/s11269-018-1928-2.

Alashan, S., 2020b. Testing and improving type 1 error performance of Şen's innovative trend analysis method. Theor. Appl. Climatol. 142 (3), 1015–1025. https://doi.org/10.1007/s00704-020-03363-5.

Alashan, S., 2024. Non-monotonic trend analysis using Mann-Kendall with self-quantiles. Theor Appl Climatol. https://doi.org/10.1007/s00704-023-04666-z.

Alashan S (2020a) Combination of modified Mann-Kendall method and Şen innovative trend analysis. Engineering Reports 2(3). https://doi. org/10.1002/eng2.12131.

Benzater B, Elouissi A, Benaricha B & Habi M (2019) Spatio-temporal trends in daily maximum rainfall in northwestern Algeria (Macta watershed case, Algeria). Arab J Geosci 12(11):1–18. https://doi. org/10.1007/s12517-019-4488-8.

Berhail, S., Katipoğlu, O.M., 2023. Comparison of the SPI and SPEI as drought assessment tools in a semi-arid region: Case of the Wadi Mekerra basin (northwest of Algeria). Theor. Appl. Climatol. 154 (3), 1373–1393. https://doi.org/10.1007/s00704-023-04601-2.

Birpınar, M.E., Kızılöz, B., Şişman, E., 2023. Classic trend analysis methods' paradoxical results and innovative trend analysis methodology with percentile ranges. Theor. Appl. Climatol. 153 (1), 1–18. https://doi.org/10.1007/s00704-023-04449-6.

Dadaser-Celik, F., Cengiz, E., Guzel, O., 2016. Trends in reference evapotranspiration in Turkey: 1975–2006. Int. J. Climatol. 36 (4), 1733–1743.

Danandeh Mehr, A., Vaheddoost, B., 2020. Identification of the trends associated with the SPI and SPEI indices across Ankara Turkey. Theor. Appl. Climatol. 139 (3), 1531–1542. https://doi.org/10.1007/s00704-019-03071-9.

Du, C., Chen, J., Nie, T., 2021. Spatial–temporal changes in meteorological and agricultural droughts in Northeast China: Change patterns, response relationships and causes. Nat. Hazards 110, 155–173. https://doi.org/10.1007/s11069-021-04940-1.

Elouissi, A., Benzater, B., Dabanli, I., Habi, M., Harizia, A., Hamimed, A., 2021. Drought investigation and trend assessment in Macta watershed (Algeria) by SPI and ITA methodology. Arab. J. Geosci. 14, 1–13. https://doi.org/10.1007/s12517-021-07670-7.

Eren, B., Yaqub, M., 2024. Analysis of short-term changes in air quality for two industrial zones by innovative polygon trend analysis. Int. J. Environ. Sci. Technol. 21 (4), 4343–4356. https://doi.org/10.1007/s13762-023-05286-w.

Güçlü, Y.S., 2018. Multiple Şen-innovative trend analyses and partial Mann-Kendall test. J. Hydrol. 566, 685–704. https://doi.org/10.1016/j.jhydrol.2018.09.034.

Güçlü, Y.S., Şişman, E., Dabanlı, İ., 2020. Innovative triangular trend analysis. Arab. J. Geosci. 13, 1–8. https://doi.org/10.1007/s12517-019-5048-y.

Gumus, V., Simsek, O., Avsaroglu, Y., Agun, B., 2021. Spatio-temporal trend analysis of drought in the GAP Region, Turkey. Nat. Hazards 109, 1759–1776. https://doi.org/10.1007/s11069-021-04897-1.

Gupta, N., Chavan, S.R., 2023. Assessment of changes in monthly streamflow using innovative polygon trend analysis in the South Indian Rivers. Arab. J. Geosci. 16 (12), 657. https://doi.org/10.1007/s12517-023-11767-6.

Helsel, D.R., Frans, L.M., 2006. Regional Kendall test for trend. Environ. Sci. Tech. 40 (13), 4066–4073. https://doi.org/10.1021/es051650b.

Kartal, V., Emiroglu, M.E., 2024. Hydrological Drought and Trend Analysis in Kızılırmak, Yeşilırmak and Sakarya Basins. Pure Appl. Geophys. 1–25 https://doi.org/10.1007/s00024-024-03499-9.

Katipoğlu, O.M., 2022. Analyzing the trend and change point in various meteorological variables in Bursa with various statistical and graphical methods. Theor. Appl. Climatol. 150 (3), 1295–1320.

Katipoğlu, O.M., Acar, R., 2022. Space-time variations of hydrological drought severities and trends in the semi-arid Euphrates Basin, Turkey. Stoch. Env. Res. Risk A. 36 (12), 4017–4040. https://doi.org/10.1007/s00477-022-02246-7.

Kendall, M.G., 1975. Rank correlation methods. Charles Griffin Book Series, London. https://doi.org/10.1007/s00704-022-04231-0.

Kesgin, E., Yaldız, S.G., Güçlü, Y.S., 2024. Spatiotemporal variability and trends of droughts in the Mediterranean coastal region of Türkiye. Int. J. Climatol.

Kömüşcü, A.Ü., Aksoy, M., 2023. Long-term spatio-temporal trends and periodicities in monthly and seasonal precipitation in Turkey. Theor. Appl. Climatol. 151 (3), 1623–1649. https://doi.org/10.1007/s00704-022-04349-1.

Körük, A.E., Kankal, M., Yıldız, M.B., Akçay, F., Şan, M., Nacar, S., 2023. Trend analysis of precipitation using innovative approaches in northwestern Turkey. Phys. Chem. Earth, Parts a/b/c 131, 103416. https://doi.org/10.1016/j.pce.2023.103416.

Koycegiz, C., 2024. Spatiotemporal analysis of precipitation variability in an endorheic basin of Turkey with coordinated regional climate downscaling experiment data. Alex. Eng. J. 91, 368–381. https://doi.org/10.1016/j.aej.2024.02.010.

Lai, C., Zhong, R., Wang, Z., Wu, X., Chen, X., Wang, P., Lian, Y., 2019. Monitoring hydrological drought using long-term satellite-based precipitation data. Sci. Total Environ. 649, 1198–1208. https://doi.org/10.1016/j.scitotenv.2018.08.245.

Mann, H.B., 1945. Nonparametric tests against trend. Econometrica 245–259.

Mckee TB, Doesken NY & Kleist Y (1993) The relationship of drought frequency and duration to time scales. In Proceedings of the 8th Conference on Applied Climatology, Anaheim, CA, USA, 17–22 January; pp. 179–184.

Milly, P.C., Betancourt, J., Falkenmark, M., Hirsch, R.M., Kundzewicz, Z.W., Lettenmaier, D.P., Stouffer, R.J., 2008. Stationarity is dead: Whither water management? Science 319 (5863), 573–574. https://doi.org/10.1126/science.1151915.

Mishra, A.K., Singh, V.P., 2010. A review of drought concepts. J. Hydrol. 391 (1–2), 202–216. https://doi.org/10.1016/j.jhydrol.2010.07.012.

Nacar, S., Şan, M., Kankal, M., Okkan, U., 2024. Innovative Polygonal Trend Analysis (IPTA) in detecting the seasonal trend behavior of statistically downscaled precipitation for the Eastern Black Sea Basin of Turkey. Urban Water J. 1–13. https://doi.org/10.1080/1573062X.2024.2312496.

Nalbantis, I., Tsakiris, G., 2009. Assessment of hydrological drought revisited. Water Resour. Manag. 23, 881–897. https://doi.org/10.1007/s11269-008-9305-1.

Nouri, M., Homaee, M., 2020. Drought trend, frequency and extremity across a wide range of climates over Iran. Meteorol. Appl. 27 (2), e1899.

Salim, D., Doudja, S.G., Ahmed, F., Omar, D., Mostafa, D., Oussama, B., Mahmoud, H., 2023. Comparative study of different discrete wavelet based neural network models for long term drought forecasting. Water Resour. Manag. 37 (3), 1401–1420. https://doi.org/10.1007/s11269-023-03432-0.

Şan, M., Akçay, F., Linh, N.T.T., Kankal, M., Pham, Q.B., 2021. Innovative and polygonal trend analyses applications for rainfall data in Vietnam. Theor. Appl. Climatol. 144, 809–822. https://doi.org/10.1007/s00704-021-03574-4.

Şan, M., Nacar, S., Kankal, M., Bayram, A., 2024. Spatiotemporal analysis of transition probabilities of wet and dry days under SSPs scenarios in the semi-arid Susurluk Basin. Türkiye. Science of the Total Environment 912, 168641. https://doi.org/10.1016/j.scitotenv.2023.168641.

Sen, P.K., 1968. Estimates of the regression coefficient based on Kendall's tau. J Am Stat Assoc 63 (324), 1379–1389.

Şen, Z., 2012. Innovative trend analysis methodology. J. Hydrol. Eng. 17 (9), 1042–1046. https://doi.org/10.1061/(ASCE)HE.1943-5584.0000556.

Şen, Z., 2014. Trend identification simulation and application. J. Hydrol. Eng. 19 (3), 635–642. https://doi.org/10.1061/(ASCE)HE.1943-5584.0000811.

Şen, Z., 2017. Innovative trend significance test and applications. Theor. Appl. Climatol. 127, 939–947. https://doi.org/10.1007/s00704-015-1681-x.

Şen, Z., Şişman, E., Dabanli, I., 2019. Innovative polygon trend analysis (IPTA) and applications. J. Hydrol. 575, 202–210. https://doi.org/10.1016/j.jhydrol.2019.05.028.

Serinaldi, F., Chebana, F., Kilsby, C.G., 2020. Dissecting innovative trend analysis. Stoch. Env. Res. Risk A. 34, 733–754. https://doi.org/10.1007/s00477-020-01797-x.

Serkendiz, H., Tatli, H., Kılıç, A., Çetin, M., Sungur, A., 2024. Analysis of drought intensity, frequency and trends using the spei in Turkey. Theor. Appl. Climatol. 155 (4), 2997–3012. https://doi.org/10.1007/s00704-023-04772-y.

Simsek, O., Ceyhunlu, A.I., Ceribasi, G., Keskiner, A.D., 2024. Evaluation of long-term meteorological drought in the aras and coruh basins with crossing empirical trend analysis. Phys. Chem. Earth, Parts a/b/c 103611. https://doi.org/10.1016/j.pce.2024.103611.

Şişman, E., Kizilöz, B., 2021. The application of piecewise ITA method in Oxford, 1870–2019. Theor. Appl. Climatol. 145, 1451–1465. https://doi.org/10.1007/s00704-021-03703-z.

Theil, H., 1950. A rank-invariant method of linear and polynomial regression analysis. Indag. Math. 12 (85), 173.

Thornthwaite, C.W., 1948. An approach toward a rational classification of climate. Geogr. Rev. 38, 55.

Tong, S., Lai, Q., Zhang, J., Bao, Y., Lusi, A., Ma, Q., Li, X., Zhang, F., 2018. Spatiotemporal drought variability on the Mongolian Plateau from 1980–2014 based on the SPEI-PM, intensity analysis and Hurst exponent. Sci. Total Environ. 615, 1557–1565. https://doi.org/10.1016/j.scitotenv.2017.09.121.

Tsakiris, G.P., Loucks, D.P., 2023. Adaptive water resources management under climate change: An introduction. Water Res. Manage. 37 (6), 2221–2233. https://doi.org/10.1007/s11269-023-03518-9.

Tsakiris, G., Pangalou, D., Vangelis, H., 2007. Regional drought assessment based on the Reconnaissance Drought Index (RDI). Water Resour. Manag. 21, 821–833. https://doi.org/10.1007/s11269-006-9105-4.

Vicente-Serrano, S.M., Beguería, S., López-Moreno, J.I., 2010. A multiscalar drought index sensitive to global warming: the standardized precipitation evapotranspiration index. J. Clim. 23 (7), 1696–1718. https://doi.org/10.1175/2009JCLI2909.1.

Von Storch H (1995) Misuses of statistical analysis in climate research. Analysis of climate variability: applications of statistical techniques. HV Storch, A. Navarra (eds.), 11-26. doi: 10.1007/978-3-662-03744-7_2.

Wilhite, D.A., 2000. Drought as a Natural Hazard: Concepts and Definitions. In: Drought: A Global Assessment. Routledge:, London, UK, pp. 3–18.

Wu, H.J., Su, X.L., Singh, V.P., Feng, K., Niu, J.P., 2021. Agricultural drought prediction based on conditional distributions of Vine Copulas. Water Resour Res 57 (8). https://doi.org/10.1029/2021WR029562 e2021WR02956.

Wu, C., Xu, Y., Jin, J., Zhou, Y., Nie, B., Li, R., Cui, Y., Tong, F., Zhang, L., 2024. Meteorological to agricultural drought propagation time analysis and driving factors recognition considering time-variant characteristics. Water Resour. Manag. 38 (3), 991–1010. https://doi.org/10.1007/s11269-023-03705-8.

Yenice, A.C., Yaqub, M., 2022. Trend analysis of temperature data using innovative polygon trend analysis and modeling by gene expression programming. Environ. Monit. Assess. 194 (8), 543.

Yeşilköy, S., Şaylan, L., 2022. Spatial and temporal drought projections of northwestern Turkey. Theor. Appl. Climatol. 149 (1), 1–14. https://doi.org/10.1007/s00704-022-04029-0.

Yuce, M.I., Deger, I.H., Esit, M., 2023. Hydrological drought analysis of Yeşilırmak Basin of Turkey by streamflow drought index (SDI) and innovative trend analysis (ITA). Theor. Appl. Climatol. 153 (3–4), 1439–1462. https://doi.org/10.1007/s00704-023-04545-7.

Yue, S., Pilon, P., Phinney, B., Cavadias, G., 2002. The influence of autocorrelation on the ability to detect trend in hydrological series. Hydrol. Process. 16 (9), 1807–1829. https://doi.org/10.1002/hyp.1095.